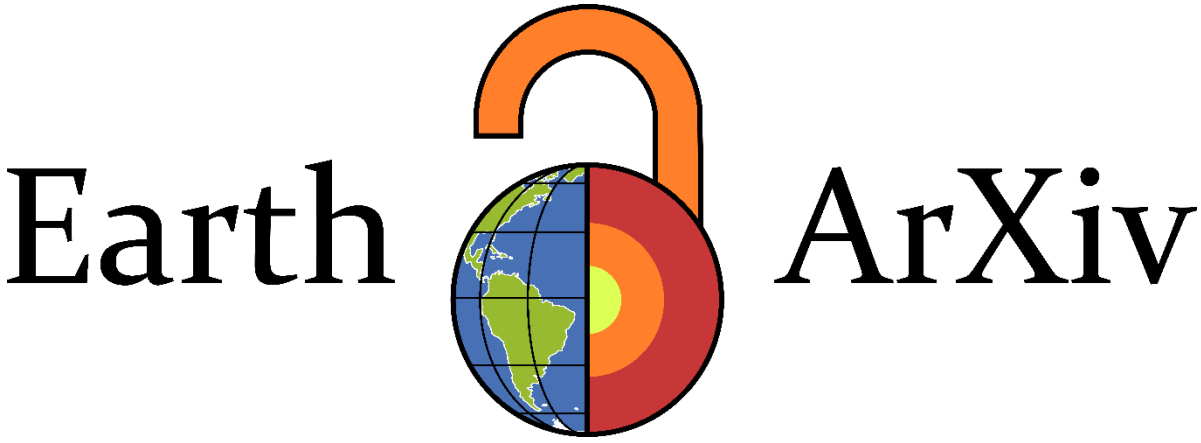

Prioritizing wildfire fuel management in California

Jing Cheng[1*], Michael L. Goulden[2], Jim Randerson[2], Shane Coffield[2], A. Park Williams[3], Qiang Zhang[4], Michael D. Mastrandrea[5], Michael W. Wara[5], and Steven J. Davis[1*]

[1] *Department of Earth System Science, Stanford University, Stanford, California, USA*
[2] *Department of Earth System Science, University of California, Irvine, California, USA*
[3] *Department of Geography, University of California, Los Angeles, California, USA*
[4] *Department of Earth System Science, Tsinghua University, Beijing, China*
[5] *Woods Institute for the Environment, Stanford University, Stanford, CA, USA*

*corresponding authors: chengj10@stanford.edu, sjdavis@stanford.edu

Main Text:
Text: 4066 words (excluding abstract, references, tables and figure captions)
Figures: 1-5

Supplementary Information:
Figures: S1- S26
Tables: S1- S12
Text: S1

The resources available for managing wildfire risk are insufficient and ultimately finite, while the risk of catastrophic fires is enormous and growing. Prioritization of responses is thus critical, but the basis for comparing the costs and societal benefits of alternative investments in wildfire mitigation is inadequate. Here, we assess and compare the costs of landscape-scale fuel treatment in California to the benefits of avoided destruction of property and smoke-related health impacts, and identify areas where the net benefits are greatest statewide. We find that re-prioritizing treatment areas could increase net benefits by a factor of more than 6.5 relative to historical treatments, with average net benefits in the top decile of areas (i.e., 28,000 km^2) of >$220k per km^2 (as compared to an estimated $90k per km^2 of past treatments). By integrating physical, epidemiological, and economic methods, our results reveal large opportunities for improving the cost-effectiveness of fuel treatments, and demonstrate a general framework that can be applied by land managers in all wildfire-prone areas. ***[165 words]***

Rising temperatures and changing precipitation have increased the size, likelihood, and intensity of California wildfires in recent decades[1-5]. At the same time, rapid growth of population and infrastructure have exposed ever more people and physical assets to harm[6,7]. The combined result has been a surge in the economic and human health impacts of wildfire in California[8], including not only the direct loss of life and destruction of infrastructure but also the impact of wildfire smoke on human health[9-13], multi-billion dollar investments in wildfire suppression[14-16], increasing costs and unavailability of insurance[17,18], rising electricity prices and disruptive power outages as utilities seek to prevent ignitions[19,20], and a loss of forest cover and associated ecosystem services[21]. In many cases, these impacts disproportionately affect vulnerable and low-income populations[22-25].

Among the proposed responses to California's wildfire emergency is to drastically increase landscape-scale management of wildfire fuels[26-28]. Common wildfire fuel treatments include mechanical thinning and prescribed burning, in each case intended to reduce the size and severity of fires by decreasing or altering the structure of vegetation[29-32]. Between 2011 and 2020, the U.S. federal and local state governments invested a combined $22.8 billion (in 2020 USD, excluding suppression investment) to treat ~133,030 km^2 (32.9 million acres), of which 50,800 km^2 (38%) were treated by mechanical or herbicide thinning, 73,150 km^2 (55%) by prescribed burning, and 9,080 km^2 (7%) by other methods[33,34]. Since 2018, the area of fuel treatments in California has averaged 2,040 km^2 per year[35], at an average cost of ~$287 million[36] per year (~$141k per km^2).

Given recent increases in catastrophic fires, the U.S. Forest Service (USFS) and California Department of Forestry and Fire Protection (CAL FIRE) plan to increase the combined scale of their treatments to ~4000 km^2 annually by 2025 (~1M acres or 1% of the state)[37]. Yet recent research has suggested that as much as 80,000 km^2 (20M acres or about 20% of the state) would benefit from sustained treatment[38], which would require decades of management even at the increased rate of treatment and ignoring regrowth. Moreover, California fire risks are spatially heterogeneous, with radically different vegetation, fire ecology, and exposed infrastructure and human population. Prioritization of the areas treated is thus critical to maximizing benefits of treatment efforts. Prior studies have evaluated the costs, applications, and limitations of different types of fuel treatments[39-44] as well as hazards to property[45-49], human life[44,50], and human health and well-being[9,51-57]. However, those that have sought to inform management priorities have generally focused on relatively detailed and localized modeling of the likelihood[58], spread risk[59], and projected severity[60,61] of wildfires; though some researchers and policymakers have begun considering priorities more broadly[62]. Here, we use a

combination of machine learning, chemical transport, and epidemiological models to systematically assess the economic costs and benefits of different types of fuel management at 0.01° × 0.01° (~1.11 km^2) resolution across California, both for the present and in 2050 under a mid-range climate change scenario (RCP4.5). We evaluate the benefits of avoided property destruction and smoke-related impacts to human health, the latter of which has rarely been included in prioritization of fuel treatments. Our analysis relies on spatially-explicit datasets of both historical and future vegetation and land cover[63-66], topography[67], canopy characteristic[68-70], climatological meteorology[71-74], building density[75-77], road density[78], population density[79,80], burn probability[81,82], fuel load[83] and moisture[84-86], fire spread rate and flame length[3,87-90], historical treatment costs[91] and the smoke emissions ($PM_{2.5}$) from wildfires[92] and prescribed burns[93-97].

Details of our data sources and analytic approach are in the *Methods*. In summary, we first estimate the cost of fuel treatments (mechanical thinning, manual thinning, prescribed burn, and other treatments; see Table S1) for each 0.01-degree grid cell statewide using a machine learning model trained on historical treatment costs and a range of physical characteristics (Fig. 1A, Fig. S1, and Table S2). We then use a similar approach to estimate the $PM_{2.5}$ emissions that would occur if a given grid cell were to burn both in its current untreated state and after treatment by the lowest-cost method. In doing so, we evaluate treatment-related changes in burn probability, fuel and canopy characteristics, and post-fire behavior based on vegetation cover-specific values collected from literature; Fig. 1B, Table S5-S6, Figs. S12-14). Next, we evaluate the damages from the $PM_{2.5}$ emissions produced in each grid cell both with and without treatment using atmospheric (GEOS-Chem) and epidemiological (BenMAP-CE[98]) models to estimate morbidity and mortality due to transported smoke given typical fire season meteorology and downwind population densities, as well as direct destruction of any buildings present (assuming that treatment could prevent the direct destruction of buildings; Fig. 1C). The economic value of health impacts is evaluated following the U.S. Environmental Protection Agency's default methods, and—importantly—we also model the health impacts of smoke from prescribed burns based on observed emissions from such managed fires and the different meteorological conditions that prevail during late winter and early spring burn windows[93-97] (see Text S1, Table S4 for details). Finally, we compare the annual (year-1) economic costs and benefits of fuel treatment in each grid cell and identify priority areas for management as those where the net benefits (i.e., less costs) are greatest. We also project changes in the cost-effectiveness of fuel treatments in 2050 under climate change (specifically the RCP4.5/SSP245 scenario in which global mean temperature increases by 2-3°C by the end of the century; see Methods and Supplementary Material for details).

Spatial distribution of fuel treatment costs and benefits

The map in Figure 2A shows spatial patterns in the lowest estimated one-time treatment costs across California (See Fig. S3 for a comparison of costs across different treatment types), ranging from as little as \$102k per km^2 (95% CI: \$89k-\$124k per km^2) up to \$4.79M per km^2 (\$4.05M-5.68M per km^2). Costs are greatest in areas with higher vegetation cover and fuel load (e.g., Del Norte and Humboldt counties; Fig. S4), steeper terrain (e.g., areas of the Sierra Nevada and Coast Ranges; Fig. S4), or more buildings (e.g., San Diego). In particular, the high population and building density and complex topography in Southern California (Fig. S4) necessitate either costly manual thinning or prescribed burns that have their own health burden, leading to higher treatment costs in the region. Even when including treatment-related damages to human health (i.e., smoke from prescribed burns) in treatments, we find that prescribed burning is the lowest-cost treatment in most areas (covering 62% of areas where the

probability of burning is greater than zero; Fig. S5, S17). However, mechanical thinning is less expensive in some cases (19% of areas with non-zero burn probability, respectively), particularly in Humboldt, Lassen, and also in Southeast counties where population densities in the wildland-urban interface increase the health-related costs of prescribed burning.

Figure 2B shows the analogous distribution of year-1 benefits of treating different areas, based on assumptions of fuel treatment efficacy on post-fire burn probability, behavior and vegetation characteristics (Table S5-S6, Figs. S12-14). Note also that the benefits shown reflect both local and remote effects, including benefits that may occur elsewhere (e.g., avoided health impacts in downwind populated areas, Fig. S6). Estimated benefits of treatment range from \$70k per km^2 (\$61k-\$81k per km^2) to \$5.88M per km^2 (\$5.35M-\$7.36M per km^2). The greatest benefits of treatment are concentrated in areas with high vegetation cover and fuel loads—where the risks of large and smoky fires are high (e.g., northwest counties and regions surrounding the Sierra Nevada), or in areas with buildings and nearby population centers (e.g., metropolitan areas of Southern California).

In turn, Figure 2C highlights the distribution of net benefits (one-time treatment costs less year-1 benefits). Overall, fuel treatments tend to be more beneficial in Northern California than Southern California, primarily contributed by the substantial health-related benefits (Fig. S7). Notably, treatment costs exceed benefits (by as much as \$462k per km^2) in many areas surrounding the Mojave Desert and mountains of eastern San Diego County, where steep, hot, and dry terrain increases costs and sparse population and property limits benefits (Fig. S4). In contrast, high burn probabilities and greater densities of population and buildings in many counties of Central and Northern coastal California and wildland-urban interfaces throughout the state correspond with substantial net benefits. Indeed, these coastal areas and wildland-urban interfaces are among the areas where the net benefits of treatment are greatest, along with areas of the heavily vegetated western Sierra Nevada slope upwind of large population centers (top 1% in Fig. 2D). Next greatest in terms of net benefits are more widespread but still heavily vegetated areas throughout the Sierra Nevada and forests of Northern California (top 10% in Fig. 2D). We note that these estimates are conservative because they compare one-time costs to the benefit in the year of treatment whereas prior work shows that risk reduction benefits for prescribed fire in particular extend for up to 8 years (Table S7-S8).

To illustrate how treatment cost-effectiveness and its drivers vary across landscapes, Figure 3 shows higher resolution maps (20 × 30 km) of three representative areas within California: a mostly-forested area of Plumas and Sierra counties (Fig. 3a), an urban area of Los Angeles (Fig. 3b), and an area with both urban development and open space near Santa Barbara (Fig. 3c). In each region, the previously treated areas (cells with black outlines in Figs. 3d-f) frequently exclude areas with the greatest estimated net benefits. Indeed, we estimate net *costs* (i.e. no net benefits) in >60% of the historical treatments in these regions of Los Angeles and Santa Barbara, while many of the areas with high projected net benefits have not been treated (Figs. 3d-3f).

The regional maps also reveal some key differences underlying the estimated net benefits. For example, areas within the Plumas-Sierra region that are among the top 10% of net benefits statewide (grid cells outlined in white) tend to be forested (i.e. dark green in Fig. 3a and dark blue in Fig. 3d), with an average of 82% of those benefits in those areas related to avoided impacts of smoke on human health (grid cells with white outlines in Fig. 3g). In contrast, those high priority areas in the mapped areas of Los Angeles and Santa Barbara have more roads and buildings (orange and red in Figs. 3b and

3c), but only slightly less (77% and 69%, respectively) benefits on average related to avoided health impacts of smoke (Figs. 3h and 3i).

There are also notable patterns in the least-cost treatment types and key cost drivers: although prescribed burning tends to be most cost-effective treatment type in forested areas, in the areas of these regions estimated to be among the top 10% of net benefits statewide (grid cells outlined in white) mechanical or manual thinning are more often preferred (76%, 64%, and 54% in Plumas-Sierra, Los Angeles, and Santa Barbara, respectively; Figs. 3j-l). Among these regions, prescribed burning is most often recommended in the highest net benefit areas of Santa Barbara (46% of the top 10% areas; Fig. 3l). Meanwhile, treatment costs in the areas with the highest net-benefits (the top 10%) tend to be most sensitive to vegetation cover in all the regions, but there is considerable variability: only 51%, 30% and 43% of such areas are most sensitive to vegetation cover in Plumas-Sierra, Los Angeles, and Santa Barbara, respectively (Figs. 3m-o).

Priority areas for treatment

Sorting treatable areas by their net benefits, we find that 60% of areas statewide have benefits greater than costs and the top 10% have net benefits greater than \$220k per km^2 (Fig. 4A). Priority areas are commonly coastal and forested (Fig. 2A, Fig. S8). Moreover, of the areas with net benefits >\$100k per km^2, 68% are federally managed and 29% are state managed[99] (yellow and purple in Fig. 4A, respectively). Table S9 gives the magnitude of these priority areas by county.

Considering what may be fixed treatment budgets, the red curve in Fig. 4B shows the cumulative estimated costs of treating areas, assuming areas with the greatest net benefits are prioritized. For example, paying for \$10B of treatment would allow the 40% of areas with the greatest net benefits to be treated, with potential benefits of \$26B (blue curve). In contrast, 26% of treatable areas have actually been treated (or have burned in wildfires) over the past 12 years, at a total treatment cost of \$14B (red circle in Fig. 4B; see also Fig. S15) with estimated benefits of \$15B (blue circle in Fig. 4B). Thus, the average net benefit-to-cost ratios of historical fuel treatments in the state is 0.1 (see grey dashed line in Fig. 4C), whereas the average ratio in areas where net benefits are in the top 10% is 10.1 (95% CI: 8.0 – 12.1); darker shaded bars in Fig. 4C). Indeed, we estimate that costs have exceeded benefits for a number of areas that have been treated in the past, in some cases by a factor of ~10 (lower deciles of net benefit in Fig. 4C).

As indicated in the results reported above and shown by shading in Fig. 4A, we calculate an overall uncertainty of roughly ±36% for net benefits. Systematically assessing the sensitivity of our results to different variables, we find that population density, fuel condition (e.g., fuel load, fuel moisture), treatment efficacy, canopy coverage and wind speed are the five most important. However, their influence on estimated net benefit varies according to the type of treatment. In the areas we identify as highest priority for treatment (i.e. the top decile), population density is the most important variable due to its influence on estimated health impacts (purple bars in Fig. 4D). But treatment efficacy, fuel loading, and canopy coverage are also quite important—especially in lower priority treatment areas—because these variables strongly affect both prevention costs and fire emissions in the machine learning model (green and blue bars in Fig. 4D).

Climate-driven changes in treatment priorities

California's meteorological conditions and vegetation cover could change substantially under future climate change, with concomitant effects on treatment costs, smoke emissions, and wildfire damage. Figure 5 shows the consequences of moderate global warming (i.e. an SSP245 scenario in which global mean temperatures rise by 2-3°C above pre-industrial levels by the end of the century) on the net benefits of fuel treatments as of 2050. Overall, average net benefits increase by 15% in the future climate relative to 2020, with maximum net benefits of $514k per km^2 and the cumulative net benefits of the top decile increasing by 27% (Fig. 5A). This is because higher temperatures, dry conditions, and slight increases in vegetation cover projected under climate change are expected to increase the frequency and severity of wildfires. These changes will increase the cost of fuel treatments, but not as much as they increase the potential benefits, especially related to human health (Fig. 5A). Note that these results assume no change in the scale or distribution of population and infrastructure; increases in exposed people and infrastructure would further increase net benefits (and perhaps alter their spatial distribution).

Despite the assumption of static exposure, regional differences in net benefits increase under climate change compared to the present. Given projected increases in the probability of wildfires in Northern California (Fig. S17), the net benefits of fuel treatment exhibit an overall northward trend, with the areas of greatest net benefits increasingly concentrated either nearby population centers or thickly forested areas of the northwestern coasts and western slope of the Sierra Nevada mountains (blue areas in Figs. 5B and 5C). In contrast, climate change will reduce the net benefits of treatments in most desert areas and large swaths of the Shasta Cascades in Siskiyou, Trinity, and Tehama counties (yellow and orange areas in Figs. 5B and 5C). The redistribution of treatment net benefits is closely correlated with projected changes in canopy coverage[64,100] and burn probability (Fig. S17).

Discussion and Conclusions

Our results reveal considerable geographical heterogeneity in the net benefits of treating wildfire fuels across California, even within a single region (see, e.g., the many neighboring orange and blue-shaded areas in Fig. 2C). In particular, by assessing the avoided damages of smoke on human health in downwind areas, high priority areas for treatment appear quite different from historical patterns of treatment. Prioritizing future treatments based on our results could immediately increase net benefits by a factor of 6.5 relative to past treatments.

The areas we identify in the top decile of net benefits are also divided almost evenly between areas of federal and state responsibility (Fig. 4A). The distribution of priority areas is thus consistent with USFS and CalFire goals to each treat about 2,000 km^2/yr (combined 4000 km^2/yr) in coming years. At this rate, the areas in the top decile of net benefits could be treated within 8 years, with annual expenditures and net benefits on the order of $42M and $375M per year, respectively (although both expenditures and net benefits might increase under climate change; Figs. 4A and 5A). Moreover, although the highest priorities are more commonly located in the northern part of the state, they are distributed among counties (Table S9). However, the greatest benefits of treatments would be concentrated in populated and/or developed areas (Fig. S4 and Fig. S6).

Our findings are subject to important uncertainties and limitations. First, although our analysis includes a rigorous evaluation of potential smoke-related health impacts and builds on state-of-the-art fire risk assessments, we make several simplifying assumptions. For example, the net benefits we report

neglect the costs of needed re-treatment (i.e. they are one-time treatment costs)[101], but also reflect only single-year benefits to human health and property. However, in a series of sensitivity analyses we show that accounting for multi-year benefits (in areas where treatment effects persist for years) has relatively little effect on the treatment priority of different areas (Figs. S10-11). For example, across these tests, the areas with the highest 1% of estimated net benefits varied by only 6%. Of course, the overall magnitude of estimated net benefits increases substantially when including multi-year benefits, which may bolster the case for larger scale treatments. It is worth noting that our assumptions about the persistence of treatments in these tests is based on dominant vegetation in different areas; future work might thus improve upon our methods by exploring and quantifying heterogeneity in retreatment costs and persistence of benefits, as well as future changes in the spatial distribution of population and buildings (which we also neglect in assessing changes in net benefits under climate change).

Second, we focus on damages to buildings and human health by smoke-related $PM_{2.5}$ if a given grid cell burns, which neglects other infrastructure (e.g., power lines, roadways, water systems), other health risks (e.g., exposure to ozone and other toxins, or the exacerbating effects of heat), and nature (e.g., endangered and symbolically important species such as giant sequoia trees, and ecosystem services such as recreation and water quality) —all productive topics for further exploration. Similarly, although our analysis incorporates spatially heterogeneous burn probabilities and treatment efficiencies, it does not capture dynamic feedbacks in fuel characteristics and wildfire risk resulting from fuel treatments and fire events. For instance, we do not model changes in burn probability due to treatments in neighboring areas or repeated wildfires. Likewise, our approach does not include ecological trade-offs in shrublands, where chaparral species typically require more than a decade to reach reproductive maturity. Frequent treatments aimed at sustaining low burn probabilities may instead trigger type conversion to invasive grasses[102,103], which can increase fire risk by promoting continuous fine fuels and faster fire spread[104-106]. Future studies would benefit from incorporating these treatment-fire interactions and ecological feedbacks to better inform landscape-scale decision-making.

In addition to assumptions and exclusions, our results are subject to methodological uncertainties related to each of the machine learning, chemical transport, and epidemiological models, as well as the underlying datasets of physical characteristics, meteorology, and historical treatment costs. For instance, the BenMAP model does not differentiate among $PM_{2.5}$ sources despite emerging evidence of important differences in the epidemiological and behavioral responses to wildfire-related $PM_{2.5}$ as compared to other sources of $PM_{2.5}$ (e.g., fossil fuel combustion)[107,108]. Wildfire-specific concentration-response functions could increase the estimated health benefits of treatments, but with little effect on the spatial distribution of net benefits. Modeling treatment costs is challenging where conditions are not well-represented in the available training data, and such extrapolations are a source of uncertainty in our results. However, >70% of the statewide variability in the features that are most important to our modeled costs and benefits are represented in the training data (Fig. S16), and our trained models skillfully predict average treatment costs (Fig. S15). The 95% confidence intervals presented throughout (e.g., Fig. 4A) and the variable sensitives in Fig. 4D reflect the results of a Monte-Carlo analysis that integrates estimates of these uncertainties. We also independently validate the machine learning and GEOS-Chem modeling procedures, and simulation results matched well with test data (see Figs. S15, S19 for costs and Figs. S18, S20 for fire emissions) and historical $PM_{2.5}$ observations (Figs. S23-S24).

Finally, there may be important and spatially heterogeneous barriers to treating different areas regardless of how high the potential net benefits are. In particular, there has sometimes been opposition

252 to prescribed burning in recent years, given the potential impacts of related smoke on human health[93]
253 and the risks that such fires will escape control of managers[94,95]. Also, there are important limitations
254 on the use of prescribed fire that are created by the Clean Air Act and state air regulation. For example,
255 the Clean Air Act in its current form treats prescribed fires—but not wildfires—as pollution sources,
256 which may limit many beneficial treatments in non-attainment areas, compounded by decreases in the
257 periods when conditions are favorable for prescribed burning (i.e., burn windows) in some parts of
258 California[95,109]. Yet our results suggest that there are large net benefits of prescribed burning despite the
259 smoke produced (as have others[96,97]). Indeed, prescribed burning is expected to be the lowest cost fuel
260 treatment over 58% of the areas in the top decile of net benefits (Fig. S3), and the total net benefits of
261 treating these areas decrease by more than $1B (from $12.3B to $11.1B) if prescribed burning were
262 disallowed. Moreover, important non-economic constraints apply to other treatment methods; manual
263 and mechanical thinning are much more labor-intensive than prescribed burning and unavailability of
264 workers could limit the area of annual treatments even more than funding in the near term[38,110]. But
265 although our analysis neglects many legal, administrative, ecological, socio-political, and logistical
266 constraints—particularly those limiting the use of prescribed fire—that may make the modeled
267 treatments impossible at the scale or in the locations where we find the greatest net benefits, decision
268 makers could nonetheless use our results to prioritize among possible treatment areas, and thereby
269 increase the social benefits of such treatments regardless of scale or local constraints.

270 Despite analytic simplifications and uncertainties, our results provide a critical new perspective for
271 decision-makers who contend with the daunting Californian reality of enormous and increasing fire
272 risks, finite resources of time, labor and funds, and vast areas needing fuel treatment. In this context,
273 methods for prioritization are a fraught necessity mostly lacking to date. By integrating physical,
274 epidemiological, and economic considerations at high spatial resolution across the entire state, we offer
275 a scientifically coherent and robust framework for valuing fuel management options at the scale of
276 states and regions in keeping with policy proposals calling for systematic evaluation of wildfire
277 mitigation options[111,112].

278 Our findings are relevant for multiple decision-making levels—from federal and state agencies such
279 as USFS and CAL FIRE, to local fire management districts and state legislators. The high-resolution
280 maps of estimated treatment costs and benefits that we present can be directly incorporated into planning
281 processes to improve the outcome of fuel treatments. Importantly, our analysis demonstrates that public
282 health benefits from smoke reduction often constitute the majority of total social benefits, especially
283 near wildland–urban interface regions. Yet these benefits have rarely been internalized in treatment
284 planning. By explicitly valuing health impacts, our framework shifts the basis of prioritization beyond
285 traditional focus areas such as structure protection and evacuation routes, revealing new high-benefit
286 zones that might otherwise be overlooked. At the same time, our framework advances academic
287 understanding of the interaction between wildfire behavior, treatment strategies, and public health
288 outcomes. Future work may introduce additional factors and nuances to this framework, but in the
289 meantime, it is already clear that near-term investments in fuel treatments can be systematically
290 prioritized to return large and greatly increased net benefits to Californians and others living in wildfire-
291 prone areas.

292

Methods

Data sources and pre-processing

Treatment cost. Historical fuel treatment data was derived from U.S. national datasets—Hazardous Fuel Treatments, which are tracked and managed by the U.S. Forest Service's Natural Resource Manager (NRM) Forest Activity Tracking System (FACTS)[91]. It records detailed activity information, including the location, area, period, measures, equipment, and cost of the hazardous fuel reductions across the conterminous United States (CONUS) since the 1930s in the form of ESRI geodatabase. We selected all treatment activities in California during 2000-2020 (a total of 406547 activities), categorized them by treatment types (Table S1) and periods (4 types × 21 years), rasterized and re-projected these 1008 layers into standard geographical longitude-latitude-projection grids with the resolution of 0.01°× 0.01°.

Meteorology. Meteorological data from 2000 to 2020 were compiled by integrating multiple sources to ensure high spatial and temporal resolution across California. Temperature, humidity, shortwave radiation, precipitation, and wind speed were primarily obtained from the GRIDMET dataset (Abatzoglou, 2013, DOI: 10.1002/joc.3413)[71], which offers gridded daily data at approximately 4 km resolution. To supplement wind directions, ERA5-Land data[72] (Muñoz Sabater, 2019, DOI: 10.24381/cds.e2161bac) from the Copernicus Climate Data Store were used for the period 2000–2013, while HRRR (High-Resolution Rapid Refresh) data[73] (Dowell et al., 2016, DOI: 10.1175/BAMS-D-13-00238.1) from NOAA were used for 2014–2020, offering hourly fields at a 3 km resolution. We clipped all these meteorological variables covering our study domain, calculated the monthly-average and annual-average values respectively, resampled (with bilinear interpolation methods) to two datasets with spatial resolutions of 0.01° × 0.01° and 0.25° × 0.3125°, respectively. Future meteorological data is derived from the GCAP2.0 model with a monthly temporal resolution and spatial resolution of 2.0°×2.5°[74]. GCAP2.0 downscaled CMIP6 experiment outputs provided future meteorology fields to drive the GEOS-Chem chemical transport model. We calculated the average meteorological variables during 2045-2049 under SSP245 climate scenarios, re-projected and bilinearly interpolated to 0.01° × 0.01° and 0.25° × 0.3125° to fit our domain.

Topography. We accessed the elevation and slope of California from a global digital elevation model (DEM) with a high resolution of 30 arc seconds[67], and then upscaled it to 0.01°× 0.01° and 0.25° × 0.3125° via bilinear interpolation. The topography of California was assumed to be consistent throughout both historical and future analyzing periods.

Land cover type. Historical land cover classification over California was collected from the National Land Cover Database (NLCD), released by U.S. Geological Survey[63]. It provides 20 types of land cover in 2001, 2006, 2011, 2016, 2019, and 2021 with resolution of 30 arcs seconds. We generated complete annual land cover over 2000-2020 (monthly variation was not considered) by nearest-neighbor interpolation temporally; re-projected and bilinearly upscaled to 0.01° × 0.01° and 0.25° × 0.3125°. Land cover in 2050 under SSP2-RCP4.5 scenario were gathered from a global 1-km PFT-based (20 plant functional types) land projection dataset, which is developed by Chen et al through combining IAM simulations and machine learning methods[64].

Canopy characteristics. Canopy coverage and height have dominated impacts on wildfire emissions and treatment costs. Historical annual canopy coverage was acquired from a sub-product of

NLCD, Tree Canopy, which provides the proportion of tree canopy in each 30 m grid cell[68]. Future canopy coverage changes by 2050 under RCP4.5 climate scenarios were collected from Rocha et al[69]., which were developed based on future land cover projections from Chen et al[64]. Historical canopy height was derived from Forest Canopy Base Height (CBH) and Canopy Height (CH) database, which is developed by LANDFIRE program, Earth Resources Observation and Science Center (EROS)[70]. LANDFIRE established a complete, nationally consistent data collection (valid in 2001, 2012, 2014, 2016, and 2020) of wildfire-related disturbance, vegetation, fuels, regime at resolution of 30m. We thus linearly interpolated to generate annual canopy height and bilinearly upscaled to 0.01° × 0.01° and 0.25° × 0.3125°. Due to limited findings on canopy height changes under climate change, we assumed CBH in 2050 keeps in line with its 2020 status.

Vegetation cover. We selected shrub, herbaceous, sagebrush, litter, and bare ground as five important vegetation classes that significantly affect wildfire emissions and treatment costs, and acquired their annual coverage over 2000-2020 from the RCMAP time-series datasets at 30-second resolution[65]. RCMAP (Rangeland Condition Monitoring Assessment and Projection) is a member of NLCD product suites, characterizing the percentage of each grid cell across Western U.S. covered by each vegetation component under the systematical methodology framework. Projections of these vegetation component coverages under RCP4.5 scenarios in 2050s were also provided by RCMAP datasets[66]. Similar to land cover data, both historical and future vegetation coverage datasets were re-projected and bilinearly upscaled to 0.01° × 0.01° and 0.25° × 0.3125°; and duplicated to 12 grids for each month regardless of monthly variation.

Burn probability. Historical wildfire burn probabilities were derived from Mann et al (https://github.com/mmann1123/WildfirePaper_PLOS1), which estimated the fire probability under the influence of human activity and climate change from 1975 to 2050 across California, with a high spatial resolution of 1080 meters[81]. However, due to the relatively outdated climate projections used in their study (i.e., CMIP3), we updated wildfire probability projections under the RCP4.5 climate change scenario from the CAL-Adapt datasets (Thomas et al., 2018[82]; https://cal-adapt.org/tools/wildfire/). This dataset provides annual wildfire simulation products for California at a spatial resolution of 0.0625 degrees, based on CMIP5 scenarios and various global climate models (GCMs). We collected decadal annual wildfire probability under the RCP4.5 scenario from 2040-2059 from four GCMs: CanESM2, CNRM-CM5, HadGEM2, and MIROC5. We then calculated the relative changes between 2040-2059 and 2000-2019; and applied the average of these relative changes from the four GCMs to the historical burn probabilities to obtain future projections. All grid datasets were bilinearly interpolated to a resolution of 0.01° × 0.01°.

Fuel characteristics. Fuel loading and fuel moisture are two critical components affecting wildfire behavior and emissions. Historical fuel loading layers were also obtained from the LANDFIRE program– Fuel Loading Models and Fuel Characteristic Classification System Fuelbeds (FCCS), which described the vegetation fuel content in each 30-m grid cell[83]. We generated monthly 0.01° × 0.01° and 0.25° × 0.3125° standard fuel loading grids over 2000-2020. We assumed the fuels in 2050 were the same as in 2020. Fuel moisture content (FMC) over the historical period was based on year 2020 data from the NCAR FMC dataset, which provides daily 1km fuel moisture grids covering CONUS[84]. From this data, we calculated the monthly mean value and bilinearly upscaled this data to our grid. Future changes in FMC of live and dead vegetation were collected from Ma et al[85] and Liu et al[86], respectively, which projected future trends of FMC under RCP4.5 climate scenarios through ecological simulations.

Fire emissions. We obtained historical wildfire emissions in California over 2000-2020 from the GFEDv4.1s database (which contains small fires) with a resolution of 0.25° × 0.25°. We obtained total dry matter emission (kg DM m^{-2} $month^{-1}$) per grid cell, and then calculated $PM_{2.5}$ emissions using emission factors in GFEDv4 database (Table S3). All historical monthly fire emission grids were bilinearly interpolated to 0.01° × 0.01°.

Fire behavior. We used conditional flame length (CFL), fire-effects flame-length probabilities (FLPs) and weighted rate of spread (wROS) as key indicators to estimate wildfire intensity and emissions. These features over 2000-2020 were derived from Pyrologix fire products, which were modelled using the FlamMap fire behavior simulation system at a spatial resolution of 30 meters[87,88]. wROS represents the weighted-average spread rate in meters per minute for a given grid cell; FLPs describes the probability distribution of fire flame lengths across six standard categories: 0–2 ft, 2–4 ft, 4–6 ft, 6–8 ft, 8–12 ft, and greater than 12 ft; and CFL characterizes the expected mean flame length for a fire burning in the direction of maximum spread at each location, assuming a fire were to occur. To account for future fire behavior, we incorporated projected changes from Loehman et al.[89] and Goss et al.[90], which simulate extreme wildfire conditions and fire regimes under the RCP4.5 climate scenario across California. Specifically, we applied projected changes in extreme fire-weather indices and high-severity fire occurrence from 2020 to the 2050s to adjust current wROS and high-flame FLPs (i.e., those exceeding 8 ft).

Building and structures. We employed three datasets, namely housing-unit density (HUDen), risk to potential structures (RPS), and structure reconstruction cost (SRC), to estimate the direct economic hazard caused by wildfires. Historical building and housing unit density and count data were obtained from Pyrologix fire products[75-77,113], which provide 30-meter resolution raster layers characterizing the built environment across the United States. HUDen expresses house-unit counts in each grid cell, generated with population and housing data from the U.S. Census Bureau, Microsoft Building Footprints data (https://hub.arcgis.com/datasets/esri::microsoft-building-footprints-features), and land cover data. RPS establishes a generic response function to characterize the potential for housing-unit damage from wildfire with an integrated consideration of fire behavior, fuel condition, and existing houses. SRC were collected from the analysis on California's estate and property by Yardi Matrix, which provides average house building costs in different counties across California (https://www.datawrapper.de/_/aoRIn/). We reprojected and bilinearly interpolated HUDen and RPS to geographic Lat/Lon 0.01° × 0.01° layers. Due to limited future projections, we assumed HUDen, RPS, and SRC would stay at the same levels.

Population. Historical population was accessed from Depsky et al.[79], which developed a high-resolution (i.e., 100-meter) population grid in California for the year of 2020 with census data; future population grids were derived from Wang et al.[80], which projected population distributions by 2100 under shared socioeconomic pathways with resolution of 1 km. We bilinearly upsampled these population grids to 0.01° × 0.01° and 0.25° × 0.3125°.

Road density. Road density data were obtained from the NOAA National Geophysical Data Center via the Data Basin repository[78] (https://databasin.org/datasets/c05cdec0ab1b4cebacbf317e7c14ed4c/). Each pixel represents the total sum length of streets and major roads (including interstate highways) within a 1 km × 1 km area, measured in meters. Following acquisition, the road density data were processed to align with the spatial framework used in this study. The original 1 km resolution data were resampled and aggregated into a uniform grid with a spatial resolution of 0.01 degrees.

Estimates of wildfire fuel treatment costs

We trained and applied Convolutional Neural Network (CNN) models to estimate fuel treatment costs across all fire-prone areas of California at 0.01° spatial resolution and annual temporal resolution. Given that different treatment activities require various fire-fighting equipment and manpower expenses, which would generate diverse treatment costs, we first categorized treatment activities into four types (i.e., prescribed fire, mechanical thinning, hand thinning, and other treatment) according to a series of characteristics[91] (e.g., treatment methods, scale and equipment features, see Table S1 for details). Then we trained CNN models for each type of activity and used the projected lowest cost among all types to represent the final treatment cost per grid cell (Fig. S3).

Four treatment-type specific CNN models were established based on a similar architecture (Fig. S2), composed of six two-dimensional convolution layers, three pooling layers, and one fully connected layer (i.e., one dense layer). All samples, including one group of predictor (Y) matrix (i.e., the recorded treatment cost), and 19 groups of driver variables (X) (Table S2), were standardized into annual 0.01° × 0.01° grids with geographic Lat/Lon projection (a total of 399 standardized grids, 19 variables × 21 years), and normalized with a min-max method.

We performed a multi-dimensional grid search approach to optimize parameter sets (including activation function, filter size, kernel size, pooling type, dropout rate, dense units, learning rate and number of epochs; Table S11) for each CNN model. Each parameter set combination was conducted 100 times of five-fold cross-validated simulations to attain the best performance with the lowest mean absolute error (MAE) and mean squared error (MSE). The final optimized CNN models were also evaluated by cross-validation with skill metrics of internal explained variance score (EV), MAE, MSE, Mean Absolute Percentage Error (MAPE), R^2, and index of agreement (IOA) (see Fig. S19 for evaluation results). We also evaluated the spatial correlation and accuracy of the predicted annual mean treatment costs by comparing them with the historical average treatment costs for each method across California during 2000–2020 (Fig. S15).

The final optimized CNN models were then applied to estimate the type-specific fuel treatment cost for current and future periods. Spatially, the prediction datasets of all driver variables cover all fire-prone areas in California with a resolution of 0.01°. In terms of temporality, we used the average estimate of each feature between 2010 and 2020 to represent the current state. We used the changes of these features around 2050 under SSP245/RCP4.5 scenarios to characterize future climate change impacts (Table S2). All CNN model training, evaluation, feature importance analysis, and projection procedures were implemented in Python (version 3.11), using the TensorFlow and Keras libraries along with standard scientific computing packages.

Projection of fire emissions

Existing fire emission databases, such as GFED[92] and Fire Modeling Intercomparison Project (FireMIP)[114], only provide emissions for the satellite era, therefore a large number of areas at risk of wildfires, at least for the same time and within a unified variable framework, do not have valid emission data. To estimate fire emissions across all fire-prone areas of California, we established fire emission machine learning models based on grid cell-specific (0.01°×0.01° and 0.25°×0.3125°) meteorological, vegetation, topography and fire behaviors using a CNN modeling architecture similar to cost estimation (Fig. S2). Then, we developed three sets of hypothetical projected monthly and seasonal wildfire

emission layers, namely wildfire emissions without fuel treatment, 1-yr post-treatment wildfire emissions, and fire emissions associated with prescribed burns, with resolution of both 0.01°×0.01° (Fig. S18) and 0.25°×0.3125°.

For wildfire emissions (including both pre- and after fuel treatment), we used variables from the wildfire season, specifically chosen from June to October based on historical wildfire activities, to construct the corresponding CNN model (CNN-WFEmis). Thus, a total of 26 groups of driver features, including meteorology, topography, land cover, vegetation, fuel characters, fire behavior and burn probability information were extracted from June through October over 2000-2020 (see *Burn probability* for details). Target variables for model training and testing were derived from GFEDv4.1s database. Both predictor and driver variables were standardized and resampled to monthly 0.01°×0.01° and 0.25°×0.3125° layers (see *Data source and pre-processing* for details). The basic framework, parameter optimization, and cross-validated evaluation process of wildfire emission CNN models are similar to cost estimation (see *Estimates of wildfire fuel treatment costs* for details). Evaluation metrics, including EV, MAE, MSE, RMSE, R^2 and IOA, of the final optimized model were assessed (see Fig. S20 for evaluation results).

Similarly, the CNN model for prescribed burns (CNN-PBEmis) was developed with the same variables but extracted from prescribed burning windows (i.e., winter and spring months, Text S1).

We then used the optimized two CNN model (CNN-WFEmis and CNN-PBEmis) to predict wildfire emissions and prescribed-burn emissions across California respectively, for the current and future periods. Prediction datasets for the current period were prepared as monthly averages of each feature through the 2010 to 2020 wildfire seasons (CNN-WFEmis) and prescribed burning windows (CNN-PBEmis), and those for future time were also collected as wildfire season averages for the 2050s under SSP245/RCP4.5 climate scenarios (Table S2).

To estimate how fuel treatments affect wildfire smoke emissions, we synthesized one-year post-treatment effects from a broad set of studies which focused on California and North America (Table S5, Figs. S12-S14). These studies report treatment-induced changes in vegetation structure (e.g., vegetation cover, canopy height, canopy bulk density), fuel load, and fire behavior indicators (e.g., burn probability, flame length). For each combination of treatment type and vegetation cover class (Fig. S4c), we calculated and summarized the mean and range of reported effects (Table S6). The mean values were used to adjust pre-treatment feature layers to represent post-treatment conditions, while the full range of estimates was applied to estimate uncertainty. These adjusted post-treatment feature layers were then input into the trained CNN-WFEmis model to predict post-treatment wildfire smoke emissions (Fig. S18). Figs. S12-S14 illustrate the spatial distributions of key features one year after applying cost-minimizing optimal treatments and their relative changes from pre-treatment conditions, respectively.

Additionally, prediction datasets for prescribed burns applied meteorological fields in prescribed burning windows, as well as reduced emission factors (Table S4, Text S1). Fig. S18 shows the spatial distribution of estimated emissions during current periods resulting from pre- and post-treatment wildfires, as well as prescribed burns. Table S10 further provides estimated primary $PM_{2.5}$ emissions originating from pre- and post-treatment fires across various fuel treatment types.

Modeling of fire-induced $PM_{2.5}$ air pollution

We employed GEOS-Chem version 13.0.0 (10.5281/zenodo.4618180) to estimate fire-specific $PM_{2.5}$ air pollution in each grid for present-day through a series of sensitivity simulations.

For wildfire-induced $PM_{2.5}$ air pollution, we performed 1014 seven-day nested GEOS-Chem simulations at a horizontal resolution of 0.25°×0.3125° and a vertical resolution of 47 layers from surface to 0.01 hPa[2]. The 1014 core simulations include one base case with all emission sources and 1013 sensitive cases that successively zero out wildfire emissions for all grids with wildfire burning probabilities. $PM_{2.5}$ air pollution caused by wildfires on a given grid was then quantified as the difference between the "all-source" simulation and the sensitive simulation zeroing out fire emissions in that grid. Considering the computational burden and the most common duration and timing of California wildfires historically (Fig. S25), we selected seven days in July to perform the 1014 core simulations.

For all 1014 core experiments, boundary conditions were dynamically provided by a global simulation with a native resolution of 2°×2.5°; chemical initial conditions employed a pre-simulated restart file using the same nested domain. Both boundary and initial conditions were simulated with all emission sources and a one-year spin-up time. We applied a 600-sec timestep for transport and a 1200-secs for the chemistry process. Meteorological input was derived from GEOS forward processing (GEOS-FP) archive, which is administered by the NASA Global Modeling and Assimilation Office (GMAO). We applied the average meteorological fields in the first week of July between 2010 and 2020 to drive all nested core simulations, in an effort to reduce meteorological uncertainty.

Emission inputs were configured with the HEMCO module[115]. Briefly, wildfire emissions were obtained from our hypothetical present-day monthly wildfire predictions and the average daily fraction factors in July between 2010 and 2020 from GFEDv4.1 database. Anthropogenic emissions for the U.S. were provided by the National Emission Inventory (NEI2011) and scaled to the average annual emission level between 2010-2020; those for other countries were provided by CEDS database[116]. Other emission sources, as from aircraft, shipping, biogenic were collected from AEIC[117], CEDS, MEGAN[118], respectively. Except for wildfire, all other emissions were applied as their average estimates of July between 2010 and 2020. We used a fully coupled NO_x-VOC-ozone-hydrocarbon-aerosol chemistry mechanism. Simulated aerosols consisted of primary black carbon, organic carbon, sea salt, dust; and secondary sulfate, nitrate, and ammonium (SNA) from the ISORROPIA II thermodynamic module. Secondary organic aerosols (SOA) were also included with a simple scheme providing a calibrated global SOA amount[119].

Considering that meteorological conditions for prescribed burns differ significantly from those in wildfires, which will have a substantial impact on $PM_{2.5}$ air pollution, we performed an additional 401 simulations to incorporate the meteorology within prescribed-burn windows. The 401 simulations include one base case with all emission sources, and 400 sensitive cases that successively zero out prescribed-burn-associated emissions for the 400 grids with the highest proportion of prescribed burns. We selected seven days in March to perform these 401 simulations. Emissions from prescribed burns were derived from our hypothetical estimates of prescribed burn emissions (see *Projection of fire emissions* for details). Except for meteorological conditions and fire emissions, all other model configurations remained consistent with the 1041 wildfire-related experiments.

Due to the core sensitivity simulations were driven by hypothetical wildfire emissions and meteorological fields, there are no valid observations or measurements that could be directly used to evaluate the model performance. Therefore, we conducted a set of benchmark experiments, including 11 one-month simulations in July between 2010 and 2020, with a 6-month spin-up time and driven by the corresponding meteorological and "all-source" emission inputs, to assess the ability of our GEOS-Chem configuration to capture daily and seasonal $PM_{2.5}$ variability in California. Observed $PM_{2.5}$ concentrations were acquired from an in-situ Air Quality System (AQS) monitoring network, which is maintained by U.S. Environmental Protection Agency (US EPA). Daily and Monthly model evaluations could be found in Fig. S23 and Fig. S24 respectively.

Indirect wildfire fuel treatment benefits

We assessed economic health benefits as indirect benefits of fuel treatment in California at 0.01° × 0.01° resolution. Here we defined the health benefit in each 0.01° wildfire-prone grid as the health benefit resulting from avoided air pollution throughout California if wildfires could be fully controlled in that grid. We integrated BenMAP-CE version 1.5[98] (Benefits Mapping and Analysis Program-Community Edition) model and Random Forest machine learning methods to quantify and downscale the monetized health benefits.

BenMAP-CE is a powerful, open-source tool to estimate the economic health impacts resulting from air quality changes (https://www.epa.gov/benmap), which has been widely used in both academia and governments. We first used BenMAP-CE to calculate the avoidable mortality associated with reducing $PM_{2.5}$ pollution as equation (1) shows.

$$\Delta Y = Y_0 \times \left(1 - e^{-\beta \Delta PM}\right) \times Pop \quad (1)$$

Where Y_0 represents the health baseline incidence. We collected county-level baseline mortality incidence rates from the Air Quality Management Plan (AQMP) Socioeconomic Analysis developed by the South Coast Air Quality Management District (SCAQMD)[120], which provided one of the most up-to-date and localized health data. ΔPM refers to changes in $PM_{2.5}$ air quality. We applied the simulated daily-average $PM_{2.5}$ concentration differences between the baseline (i.e., 'all-source') and 1013 sensitivity cases (i.e., zeroing out wildfire emissions in each fire-prone grid cell, see *Modeling of wildfire-induced $PM_{2.5}$ air pollution* for details), thus a total of 1013 BenMAP simulations were performed at a resolution of 0.25° × 0.3125°. Pop indicates the number of people = exposed to $PM_{2.5}$ air pollution. We employed the 100-meter population grid in California developed by Depsky et al[79]. (see *Data source and pre-processing* for details) here and resampled it to 0.25° × 0.3125°. β describes the health effects, namely the relation between air pollution changes and health outcomes, and is often quantified with concentration-response functions (CFs) derived from epidemiology studies. CRFs and relative risks (RR) were derived from epidemiological literatures[121-124], also natively embedded in BenMAP-CE.

The monetary value of the health effects was then estimated with willingness-to-pay valuation functions for mortality and morbidity based on the literature[125-128]. We applied a value of statistical life (VSL) for avoidable mortality of $10.3 million ($6.2–$14.5 million) adjusted to 2016 USD based on 2016 income levels. Valuation for morbidity was provided by BenMAP-CE database.

Health benefit outcomes by BenMAP-CE provided 1013 valid data points. Together with the related wildfire emission, meteorology, topography, vegetation, fuel condition, fire behavior, and

socioeconomic layers, we developed a health-related CNN model using the similar architecture (Fig. S2) to technologically downscale the coarse resolution (i.e., 0.25° × 0.3125°) to 0.01° × 0.01°, as well as project its future variation under climate changes.

Simulated monetary health benefits in 1013 coarse grids for wildfires and 400 coarse grids for prescribed burns were used as target variables to train and validate the CNN model. We employed a group of 16 driver variables (Table S2), and extracted them from their corresponding 0.25° × 0.3125° layers (see *Data source and pre-processing* for details). It is important to note that wildfire emissions in a specific grid would affect health losses in its surrounding areas, and in turn, the health benefits of that grid would also be affected by the fuel treatment of its neighbors. Therefore, apart from the 16 driver variables in each core grid, we added transport- and socioeconomic-related X drivers, such as 10-m zonal, 10-m meridional wind, population in each of the 8 grids adjacent to the core grid, as well as the average of three peripheral layers of the core grid in 8 directions (Fig. S26) in training variables as well. The model framework, optimization and evaluation process of health benefit CNN model is similar to cost estimation (see *Estimates of wildfire fuel treatment costs* for details).

Using the optimized CNN model, we downscaled the present-day health benefit grid into 0.01° × 0.01° with 0.01° projection datasets. The indirect benefits of fuel treatments were ultimately estimated as the health losses avoided between wildfire burnings and post-fire burnings, as Equation 2 shows. Apart from conventional evaluation metrics, we additionally compared the differences between CNN downscaling and bilinear interpolation, which indicated relatively close spatial distributions. Finally, driven by projection datasets in 2050 (see *Data source and pre-processing* and Table S2 for details), we predicted future health benefits of fuel treatment under SSP245/RCP4.5 climate change scenarios.

$$IBen = \sum_{i=1}^{n} (\Delta Y_{Wildfire_i} - \Delta Y_{Post-fire_i}) \times VSL \quad (2)$$

Direct wildfire fuel treatment benefits

We estimated the avoidable reconstruction and repair costs of houses that would be damaged by wildfires as the direct benefit of fuel treatments. Three sets of data, namely housing-unit counts (HU), conditional risk to potential structures (RPS), and structure reconstruction cost (SRC) (see *Data source and pre-processing* for details) were applied to quantify direct benefits as Equation 3 shows.

$$DBen = \sum_{i=1}^{n} (HU_i \times SRC_c) \times (RPS_{Wildfirei} - RPS_{Post-firei}) \quad (3)$$

Where HU_i represents the count of house unit in grid i. $RPS_{Wildfirei}$ and $RPS_{Post-firei}$ depict the potential consequences of pre- and post-treatment wildfires to a house unit at grid i, if a fire occurs there and if a home were located there. SRC_c refers to the average total reconstruction cost per building in county c.

Feature importance and uncertainty estimates

For each CNN model used in the analysis, including treatment-specific cost models and wildfire or prescribed burn emission models, we applied SHAP (SHapley Additive exPlanations)[129] to interpret the predictions of CNNs trained to estimate treatment costs by activity types, as well as fire emissions. For each specific CNN model, we conducted both model-agnostic and surrogate-based SHAP analyses to

assess the relative importance of input features. For model-agnostic interpretation, we used SHAP's Kernel Explainer to directly estimate Shapley values from the trained CNN of each treatment type. We performed ten independent runs per model, each based on 2,000 randomly selected samples, and averaged the absolute SHAP values across runs to obtain stable estimates of feature importance. Meanwhile, we trained a Gradient Boosting Regressor to approximate each CNN's predictions and applied Tree Explainer to compute SHAP values over the full training dataset. This surrogate-based approach enables efficient estimation while maintaining consistency with the CNN outputs. Feature importance was then ranked based on the mean absolute SHAP values from both explainers, as shown in Fig. S21 for treatment costs and Fig. S22 for fire emissions.

For the full modeling framework (Fig. 1; Fig. S1), we performed Monte Carlo simulations to capture both the aggregate uncertainty in model predictions and the sensitivity of outcomes to individual input features (Fig. 4). Specifically, to evaluate the influence of each feature, we adopted a feature perturbation approach based on model performance degradation. For each simulation, we randomly shuffled the values of a single input feature across the test dataset—effectively disrupting the information that feature provides—while keeping all other features unchanged. We then recorded the resulting change in the model's mean absolute error (MAE). This process was repeated for each feature across all 5,000 runs. The magnitude of the increase in MAE reflects the model's dependence on that feature: a larger rise indicates greater predictive importance.

Data and materials availability

All datasets used in this study are publicly available. (1) Historical fuel treatment records were obtained from the U.S. Forest Service FACTS system (https://data.fs.usda.gov/geodata/edw/datasets. php). (2) Meteorological data were compiled from several sources: GRIDMET daily climate data (https://www.climatologylab.org/gridmet.html), ERA5-Land reanalysis from the Copernicus Climate Data Store (https://cds.climate.copernicus.eu/cdsapp#!/dataset/reanalysis-era5-land), and HRRR hourly meteorological fields from NOAA (https://registry.opendata.aws/noaa-hrrr-pds/). Future meteorology projections were derived from GCAP2.0 downscaled CMIP6 climate fields (http://atmos.earth.rochester.edu/input/gc/ExtData/GCAP2/). (3) Topography data came from the GTOPO30 global digital elevation model (https://www.usgs.gov/centers/eros/science/usgs-eros archive-digital-elevation-global-30-arc-second-elevation-gtopo30). (4) Land cover data were obtained from NLCD (https://doi.org/10.5066/P9JZ7AO3) and future projections from Zenodo (https://zenodo.org/records/4584775). (5) Vegetation coverage datasets were from RCMAP for historical (https://doi.org/10.5066/P9SJXUI1) and projected (https://doi.org/10.5066/P134RA6V) periods. Tree canopy coverage was derived from NLCD Tree Canopy (https://www.mrlc.gov/data), and canopy height from LANDFIRE (https://landfire.gov/cbh.php), with future projections from Zenodo (https://doi.org/10.5281/zenodo.6502865). (6) Historical wildfire burn probabilities were obtained from Mann et al. (https://github.com/mmann1123/WildfirePaper_PLOS1) and future probabilities from CAL-Adapt (https://cal-adapt.org/data/download/). (7) Fuel loading and moisture data were from LANDFIRE (https://www.landfire.gov/flm.php) and NCAR FMC (https://doi.org/10.5065/qt42-zd40), respectively. (8) Fire emissions were derived from the GFEDv4.1s database (https://www.geo.vu.nl/~gwerf/GFED/GFED4/). (9) Fire behavior indicators were obtained from Pyrologix (https://pyrologix.com/downloads). Socioeconomic data including population (https://zenodo.org/records/5874927, https://doi.org/10.6084/m9.figshare.19608594.v2), road density (https://databasin.org/datasets/c05cdec0ab1b4cebacbf317e7c14ed4c), housing data and structure risk (https://pyrologix.com/downloads), building cost (https://www.datawrapper.de/aoRIn/), and baseline mortality (https://population.un.org/wpp/) were also publicly available. (10) Air quality simulations were

660 performed using GEOS-Chem v13.0.0 (https://doi.org/10.5281/zenodo.4618180), and health impact assessments
661 were conducted using BenMAP-CE version 1.5 (https://www.epa.gov/benmap/benmap-downloads).

References and Notes

1 Williams, A. P. *et al.* Observed Impacts of Anthropogenic Climate Change on Wildfire in California. *Earth's Future* **7**, 892-910, doi:10.1029/2019ef001210 (2019).

2 Goss, M. *et al.* Climate change is increasing the likelihood of extreme autumn wildfire conditions across California. *Environ. Res. Lett.* **15**, doi:10.1088/1748-9326/ab83a7 (2020).

3 Turco, M. *et al.* Anthropogenic climate change impacts exacerbate summer forest fires in California. *Proc Natl Acad Sci U S A* **120**, e2213815120, doi:10.1073/pnas.2213815120 (2023).

4 Brown, P. T. *et al.* Climate warming increases extreme daily wildfire growth risk in California. *Nature* **621**, 760–766, doi:10.1038/s41586-023-06444-3 (2023).

5 Cunningham, C. X. *et al.* Wildfires will intensify in the wildland-urban interface under near-term warming. *Commun Earth Environ* **6**, 542, doi:10.1038/s43247-025-02475-y (2025).

6 Burke, M. *et al.* The changing risk and burden of wildfire in the United States. *Proc Natl Acad Sci U S A* **118**, doi:10.1073/pnas.2011048118 (2021).

7 Modaresi Rad, A. *et al.* Social vulnerability of the people exposed to wildfires in U.S. West Coast states. *Sci. Adv.* **9**, eadh4615, doi:10.1126/sciadv.adh4615 (2023).

8 Buechi, H., Weber, P., Heard, S., Cameron, D. & Plantinga, A. J. Long-term trends in wildfire damages in California. *Int. J. Wildland Fire* **30**, 757-762, doi:10.1071/wf21024 (2021).

9 Wang, D. *et al.* Economic footprint of California wildfires in 2018. *Nat. Sustain.* **4**, 252-260, doi:10.1038/s41893-020-00646-7 (2020).

10 Aguilera, R., Corringham, T., Gershunov, A. & Benmarhnia, T. Wildfire smoke impacts respiratory health more than fine particles from other sources: observational evidence from Southern California. *Nat. Commun.* **12**, 1493, doi:10.1038/s41467-021-21708-0 (2021).

11 Heaney, A. *et al.* Impacts of Fine Particulate Matter From Wildfire Smoke on Respiratory and Cardiovascular Health in California. *Geohealth* **6**, e2021GH000578, doi:10.1029/2021GH000578 (2022).

12 Heft-Neal, S., Driscoll, A., Yang, W., Shaw, G. & Burke, M. Associations between wildfire smoke exposure during pregnancy and risk of preterm birth in California. *Environ. Res.* **203**, 111872, doi:10.1016/j.envres.2021.111872 (2022).

13 Gould, C. F. *et al.* Health Effects of Wildfire Smoke Exposure. *Annu. Rev. Med.*, doi:10.1146/annurev-med-052422-020909 (2023).

14 National Interagency Fire Center. *Federal Firefighting Costs (Suppression Only)*, https://www.nifc.gov/fire-information/statistics/suppression-costs, (National Interagency Fire Center, 2023).

15 Legislative Analyst's Office. *State Wildfire Response Costs Estimated to Be Higher Than Budgeted*. (The California Legislature's Nonpartisan Fiscal and Policy Advisor, 2020).

16 Teresa J. Feo *et al. The Costs of Wildfire in California: An Independent Review of Scientific and Technical Information*. (California Council on Science and Technology, 2020).

17 Auer, M. R. & Hexamer, B. E. Income and Insurability as Factors in Wildfire Risk. *Forests* **13**, doi:10.3390/f13071130 (2022).

18 Hazra, D. & Gallagher, P. Role of insurance in wildfire risk mitigation. *Economic Modelling* **108**, doi:10.1016/j.econmod.2022.105768 (2022).

19 Mitchell, J. W. Analysis of utility wildfire risk assessments and mitigations in California. *Fire Saf. J.* **140**, doi:10.1016/j.firesaf.2023.103879 (2023).

20 Larry Dale, Michael Carnall, Max Wei, Gary Fitts & McDonald, S. L. *Assessing the Impact of Wildfires on the California Electricity Grid-A Report for California's Fourth Climate Change Assessment*. Report No. CCCA4-CEC-2018-002, (California Energy Commission, 2018).

21 Wang, J.A., Randerson, J.T., Goulden, M.L., Knight, C. & Battles. J.J. Losses of tree cover in California driven by increasing fire disturbance and climate stress. *AGU Advances* **3(4)**: e2021AV000654, doi: 10.1029/2021AV000654 (2022).

22 Masri, S., Scaduto, E., Jin, Y. & Wu, J. Disproportionate Impacts of Wildfires among Elderly and Low-Income Communities in California from 2000-2020. *Int. J. Environ. Res. Public Health* **18**, doi:10.3390/ijerph18083921 (2021).

23 Auer, M. R. Considering equity in wildfire protection. *Sustain. Sci.* **16**, 2163-2169, doi:10.1007/s11625-021-01024-8 (2021).

24 An-Vo, D.-A., Hino, M. & Field, C. B. Fire frequency and vulnerability in California. *PLOS Climate* **2**, doi:10.1371/journal.pclm.0000087 (2023).

25 Anderson, S. E., Plantinga, A. J. & Wibbenmeyer, M. Inequality in Agency Response: Evidence from Salient Wildfire Events. *The Journal of Politics* **85**, 625-639, doi:10.1086/722044 (2023).

26 USDA Forest Service News Release. *USDA Forest Service announces landscape scale investments to restore forests across tribal, state, and privately managed lands*. (U. S. Department of Agriculture, 2023).

27 Wara, M. *A New Strategy for Addressing the Wildfire Epidmic in California* (Stanford Woods Institute Climate and Energy Policy Program White Paper, 2021).

28 Friedman, S. *Landscape-level Fire Management in California: Getting to Yes. National Forest News and Views*. (National Forest News and Views, 2021).

29 Fernandes, P. M. & Botelho, H. S. A review of prescribed burning effectiveness in fire hazard reduction. *Int. J. Wildland Fire* **12**, 117-128, doi:https://doi.org/10.1071/WF02042 (2003).

30 Agee, J. K. & Skinner, C. N. Basic principles of forest fuel reduction treatments. *For. Ecol. Manage.* **211**, 83-96, doi:10.1016/j.foreco.2005.01.034 (2005).

31 Kalies, E. L. & Yocom Kent, L. L. Tamm Review: Are fuel treatments effective at achieving ecological and social objectives? A systematic review. *For. Ecol. Manage.* **375**, 84-95, doi:10.1016/j.foreco.2016.05.021 (2016).

32 Ott, J. E., Kilkenny, F. F. & Jain, T. B. Fuel treatment effectiveness at the landscape scale: a systematic review of simulation studies comparing treatment scenarios in North America. *Fire Ecology* **19**, doi:10.1186/s42408-022-00163-2 (2023).

33 Forests and Rangelands. *Federal Wildland Fire Fuels Management Accomplishments Fiscal Years (FY) 2003-2022, Fuels Treatment Accomplishment Reports - USDA FS and USDI*. (USDA Forest Service; Department of the Interior, 2023).

34 Riddle A. A. *Federal Wildfire Management: Ten-Year Funding Trends and Issues (FY2011-FY2020),* CRS Reports No. R46583. (Congressional Research Service, 2020).

35 CAL FIRE. *CAL FIRE Fuel Reduction Projects*. https://experience.arcgis.com/experience/dfb8672f201145a4a8bf04cd9d3e37c1. (CAL FIRE, 2023).

36 Newsom, G. *Governor's Proposed Budget, the state of California, 2017-2023*. https://ebudget.ca.gov. (USDA Forest Service; Department of the Interior, 2023).

37 Newsom, G., Crowfoot, W., Blumenfeld, J. & Porter, T. *California's Wildfire and Forest Resilience Action Plan: A Comprehensive Strategy of the Governor's Forest Management Task Force*. (California Wildfire & Forest Resilience Task Force, California Department of Water Resources, Public Affairs Office, Creative Services Branch, 2021).

38 Miller, R. K., Field, C. B. & Mach, K. J. Barriers and enablers for prescribed burns for wildfire management in California. *Nat. Sustain.* **3**, 101-109, doi:10.1038/s41893-019-0451-7 (2020).

39 Thompson, M. P., Vaillant, N. M., Haas, J. R., Gebert, K. M. & Stockmann, K. D. Quantifying the Potential Impacts of Fuel Treatments on Wildfire Suppression Costs. *J. For.* **111**, 49-58, doi:10.5849/jof.12-027 (2013).

40 Taylor, M. H., Rollins, K., Kobayashi, M. & Tausch, R. J. The economics of fuel management: wildfire, invasive plants, and the dynamics of sagebrush rangelands in the western United States. *J. Environ. Manage* **126**, 157-173, doi:10.1016/j.jenvman.2013.03.044 (2013).

41 Alcasena, F., Ager, A. A., Belavenutti, P., Krawchuk, M. & Day, M. A. Contrasting the efficiency of landscape versus community protection fuel treatment strategies to reduce wildfire exposure and risk. *J. Environ. Manage* **309**, 114650, doi:10.1016/j.jenvman.2022.114650 (2022).

42 Thompson, M., Riley, K., Loeffler, D. & Haas, J. Modeling Fuel Treatment Leverage: Encounter Rates, Risk Reduction, and Suppression Cost Impacts. *Forests* **8**, doi:10.3390/f8120469 (2017).

43 Holland, T. *et al.* The management costs of alternative forest management strategies in the Lake Tahoe Basin. *Ecology and Society* **27**, doi:10.5751/es-13481-270443 (2022).

44 Thomas, D., Butry, D., Gilbert, S., Webb, D. & Fung, J. *The Costs and Losses of Wildfires, NIST Special Publication 1215*. (National Institute of Standards and Technology, U.S. Department of Commerce, 2017).

45 Price, O. F. & Bedward, M. Using a statistical model of past wildfire spread to quantify and map the likelihood of fire reaching assets and prioritise fuel treatments. *Int. J. Wildland Fire* **29**, doi:10.1071/wf18130 (2020).

46 Ager, A. A., Vaillant, N. M. & Finney, M. A. A comparison of landscape fuel treatment strategies to mitigate wildland fire risk in the urban interface and preserve old forest structure. *For. Ecol. Manage.* **259**, 1556-1570, doi:10.1016/j.foreco.2010.01.032 (2010).

47 Dale, L., Carnall, M., Fitts, G., Lewis, S. M. & Wei, M. *Assessing the Impact of Wildfires on the California Electricity Grid, A Report for California's Fourth Climate Change Assessment*. (California Energy Commission, 2018).

48 Moftakhari, H. & AghaKouchak, A. Increasing exposure of energy infrastructure to compound hazards: cascading wildfires and extreme rainfall. *Environ. Res. Lett.* **14**, doi:10.1088/1748-9326/ab41a6 (2019).

49 Hallema, D. W. *et al.* Burned forests impact water supplies. *Nat. Commun* **9**, 1307, doi:10.1038/s41467-018-03735-6 (2018).

50 Salis, M. *et al.* Evaluating alternative fuel treatment strategies to reduce wildfire losses in a Mediterranean area. *For. Ecol. Manage.* **368**, 207-221, doi:10.1016/j.foreco.2016.03.009 (2016).

51 Ye, T. *et al.* Short-term exposure to wildfire-related $PM_{2.5}$ increases mortality risks and burdens in Brazil. *Nat. Commun* **13**, 7651, doi:10.1038/s41467-022-35326-x (2022).

52 Burke, M. *et al.* The contribution of wildfire to $PM_{2.5}$ trends in the USA. *Nature*, doi:10.1038/s41586-023-06522-6 (2023).

53 Richardson, L. A., Champ, P. A. & Loomis, J. B. The hidden cost of wildfires: Economic valuation of health effects of wildfire smoke exposure in Southern California. *Journal of Forest Economics* **18**, 14-35, doi:10.1016/j.jfe.2011.05.002 (2012).

54 Koman, P. D. *et al.* Mapping Modeled Exposure of Wildland Fire Smoke for Human Health Studies in California. *Atmosphere (Basel)* **10**, doi:10.3390/atmos10060308 (2019).

55 Masri, S., Jin, Y. & Wu, J. Compound Risk of Air Pollution and Heat Days and the Influence of Wildfire by SES across California, 2018–2020: Implications for Environmental Justice in the Context of Climate Change. *Climate* **10**, doi:10.3390/cli10100145 (2022).

56 Reid, C. E. *et al.* Associations between respiratory health and ozone and fine particulate matter during a wildfire event. *Environ. Int.* **129**, 291-298, doi:10.1016/j.envint.2019.04.033 (2019).

57 Bansal, A. *et al.* Heatwaves and wildfires suffocate our healthy start to life: time to assess impact and take action. *Lancet Planet Health* **7**, e718-e725, doi:10.1016/S2542-5196(23)00134-1 (2023).

58 Chung, W. Optimizing Fuel Treatments to Reduce Wildland Fire Risk. *Current Forestry Reports* **1**, 44-51, doi:10.1007/s40725-015-0005-9 (2015).

59 Finney, M. A. Design of Regular Landscape Fuel Treatment Patterns for Modifying Fire Growth and Behavior. *For. Sci.* **47**, 219-228, doi:10.1093/forestscience/47.2.219 (2001).

60 Krofcheck, D. J., Hurteau, M. D., Scheller, R. M. & Loudermilk, E. L. Prioritizing forest fuels treatments based on the probability of high-severity fire restores adaptive capacity in Sierran forests. *Glob. Chang. Biol.* **24**, 729-737, doi:10.1111/gcb.13913 (2018).

61 Tubbesing, C. L. *et al.* Strategically placed landscape fuel treatments decrease fire severity and promote recovery in the northern Sierra Nevada. *For. Ecol. Manage.* **436**, 45-55, doi:10.1016/j.foreco.2019.01.010 (2019).

62 Alcasena, F., Ager, A. A., Belavenutti, P., Krawchuk, M. & Day, M. A. Contrasting the efficiency of landscape versus community protection fuel treatment strategies to reduce wildfire exposure and risk. *J. Environ Manage* **309**, 114650, doi:10.1016/j.jenvman.2022.114650 (2022).

63 Dewitz, J. *National Land Cover Database (NLCD) 2021 Products: U.S. Geological Survey data release.* https://doi.org/10.5066/P9JZ7AO3. (U.S. Geological Survey, 2023).

64 Chen, G., Li, X. & Liu, X. Global land projection based on plant functional types with a 1-km resolution under socio-climatic scenarios. *Sci. Data* **9**, 125, doi:10.1038/s41597-022-01208-6 (2022).

65 Shi, H., Rigge, M., Postma, K. & Bunde, B. Trends analysis of rangeland condition monitoring assessment and projection (RCMAP) fractional component time series (1985–2020). *GIScience & Remote Sensing* **59**, 1243-1265, doi:10.1080/15481603.2022.2104786 (2022).

66 Rigge, M., Postma, K., Bunde, B. & Shi, H. *Projections of Rangeland Fractional Component Cover Across Western US Rangelands for Representative Concentration Pathways (RCP) 4.5 and 8.5 Scenarios for the 2020s, 2050s, and 2080s Time-Periods: U.S. Geological Survey data release.* (U.S. Geological Survey, 2023).

67 Earth Resources Observation and Science (EROS) Center, U. S. Geological Survey. *Global 30 Arc-Second Elevation (GTOPO30).* https://www.usgs.gov/centers/eros/science/usgs-eros-archive-digital-elevation-global-30-arc-second-elevation-gtopo30?qtscience_center_objects=0 #overview (Earth Resources Observation and Science (EROS) Center & U. S. Geological Survey, 2018).

68 Geospatial Technology and Applications Center (GTAC), U.S. Department of Agriculture. *National Land Cover Database Tree Canopy Cover.* (GTAC, U.S. Department of Agriculture, 2023).

69 Rocha, T. C. *Forest land under different scenarios of future global change*. doi:10.5281/zenodo.6502865 (2022).

70 LANDFIRE, Earth Resources Observation and Science Center (EROS). *LANDFIRE Limited Update Forest Canopy Base Height (CBH) CONUS.* https://www.landfire.gov. (U.S. Geological Survey, 2021).

71 Abatzoglou, J.T. Development of gridded surface meteorological data for ecological applications and modelling. *Int. J. Climatol.*, **33**: 121-131, doi:10.1002/joc.3413 (2013).

72 Muñoz Sabater, J. *ERA5-Land hourly data from 1950 to present*. doi:10.24381/cds.e2161bac. (Copernicus Climate Change Service Climate Data Store, 2019).

73 Dowell, D. C. *et al*. The High-Resolution Rapid Refresh (HRRR): An Hourly Updating Convection-Allowing Forecast Model. Part I: Motivation and System Description. *Weather and Forecasting* **37**, 1371-1395, doi:10.1175/waf-d-21-0151.1 (2022).

74 Murray, L. T., Leibensperger, E. M., Orbe, C., Mickley, L. J. & Sulprizio, M. GCAP 2.0: a global 3-D chemical-transport model framework for past, present, and future climate scenarios. *Geoscientific Model Development* **14**, 5789-5823, doi:10.5194/gmd-14-5789-2021 (2021).

75 Scott, J. H. *et al. Wildfire Risk to Communities: Spatial datasets of landscape-wide wildfire risk components for the United States-Housing Unit Density raster for California.* (CO: Forest Service Research Data Archive Fort Collins, 2020).

76 Scott, J. H. *et al. Wildfire Risk to Communities: Spatial datasets of landscape-wide wildfire risk components for the United States-Building Exposure Type raster for California.* (CO: Forest Service Research Data Archive Fort Collins, 2020).

77 Scott, J. H. *et al. Hazard Assessment: Risk to Potential Structures raster (RPS).* (Pyrologix, 2021).

78 Conservation Biology Institute. *Road density (length in meters/sq. kilometer) for the contiguous U.S.* https://databasin.org/datasets/c05cdec0ab1b4cebacbf317e7c14ed4c/. (NOAA National Geophysical Data Center, 2011).

79 Depsky, N. J., Cushing, L. & Morello-Frosch, R. High-resolution gridded estimates of population sociodemographics from the 2020 census in California. *PLoS One* **17**, e0270746, doi:10.1371/journal.pone.0270746 (2022).

80 Wang, X., Meng, X. & Long, Y. Projecting 1 km-grid population distributions from 2020 to 2100 globally under shared socioeconomic pathways. *Sci. Data* **9**, doi:10.1038/s41597-022-01675-x (2022).

81 Mann, M. L. *et al.* Incorporating Anthropogenic Influences into Fire Probability Models: Effects of Human Activity and Climate Change on Fire Activity in California. *PLoS One* **11**, e0153589, doi:10.1371/journal.pone.0153589 (2016).

82 Thomas, N., Mukhtyar, S., Galey, B. & Kelly, M. Cal-Adapt: Linking Climate Science with Energy Sector Resilience and Practitioner Need. California's Fourth Climate Change Assessment. (California Energy Commission, 2018).

83 LANDFIRE, Earth Resources Observation and Science Center (EROS). *Fuel Characteristic Classification System (FCCS) Fuelbeds (LF 2023).* https://www.landfire.gov/fccs.php. (U.S. Geological Survey, 2024).

84 Branko Kosovic *et al. Fuel Moisture Content (Live and Dead) over the Conterminous United States. Version 1.0.* https://doi.org/10.5065/qt42-zd40. (UCAR/NCAR - GDEX, 2019).

85 Ma, W. *et al.* Assessing climate change impacts on live fuel moisture and wildfire risk using a hydrodynamic vegetation model. *Biogeosciences* **18**, 4005-4020, doi:10.5194/bg-18-4005-2021 (2021).

86 Liu, Y. Responses of dead forest fuel moisture to climate change. *Ecohydrology* **10**, doi:10.1002/eco.1760 (2016).

87 Scott, J. H. *et al. Fire behavior modeling: Weighted rate of spread (wROS).* (Pyrologix, 2021).

88 Scott, J. H. *et al. Fire behavior modeling: Fire-effects flame-length probabilities (FLPs).* (Pyrologix, 2021).

89 Loehman, R., Flatley, W., Holsinger, L. & Thode, A. Can Land Management Buffer Impacts of Climate Changes and Altered Fire Regimes on Ecosystems of the Southwestern United States? *Forests* **9**, doi:10.3390/f9040192 (2018).

90 Goss, M. *et al.* Climate change is increasing the likelihood of extreme autumn wildfire conditions across California. *Environ. Res. Lett.* **15**, doi:10.1088/1748-9326/ab83a7 (2020).

91 U.S. Forest Service. *Hazardous Fuel Treatment Reduction*. http://data.fs.usda.gov/geodata/edw/datasets.php. (U.S. Forest Service, 2023).

92 van der Werf, G. R. *et al.* Global fire emissions estimates during 1997–2016. *Earth Syst. Sci. Data* **9**, 697-720, doi:10.5194/essd-9-697-2017 (2017).

93 Kiely, L. *et al.* California Case Study of Wildfires and Prescribed Burns: $PM_{(2.5)}$ Emissions, Concentrations, and Implications for Human Health. *Environ Sci Technol* **58**, 5210-5219, doi:10.1021/acs.est.3c06421 (2024).

94 Yoder. J. Liability, Regulation, and Endogenous Risk: The Incidence and Severity of Escaped Prescribed Fires in the United States. *Journal of Law and Economics* **51**, 297-325, doi:10.1086/589661 (2008).

95 John R. Weir *et al. Prescribed Burning: Spotfires and Escapes.* (Oklahoma Cooperative Extension Service, Oklahoma State University, 2017).

96 Baijnath-Rodino, J. A. *et al.* Historical seasonal changes in prescribed burn windows in California. *Sci. Total Environ.* **836**, 155723, doi:10.1016/j.scitotenv.2022.155723 (2022).

97 Altshuler, S. L. *et al.* Wildfire and prescribed burning impacts on air quality in the United States. *J. Air Waste Manag. Assoc.* **70**, 961-970, doi:10.1080/10962247.2020.1813217 (2020).

98 Sacks, J. D. *et al.* The Environmental Benefits Mapping and Analysis Program – Community Edition (BenMAP–CE): A tool to estimate the health and economic benefits of reducing air pollution. *Environ. Model. Softw.* **104**, 118-129, doi:10.1016/j.envsoft.2018.02.009 (2018).

99 CAL FIRE. *State Responsibility Areas for Fire Protection*. https://gis.data.ca.gov/datasets/ CALFIRE-Forestry: california-state-responsibility-areas/explore. (CAL FIRE, 2023).

100 Weber, J. *et al.* Chemistry-albedo feedbacks offset up to a third of forestation's CO_2 removal benefits. *Science* **383**, 860-864, doi:10.1126/science.adg6196 (2024).

101 Wu, X., Sverdrup, E., Mastrandrea, M. D., M. W. & Wager, S. Low-intensity fires mitigate the risk of high-intensity wildfires in California's forests. *Sci. Adv.* **9**, eadi4123, doi: 10.1126/sciadv.adi4123 (2023).

102 Syphard, A. D., T. J. Brennan, and J. E. Keeley. Extent and drivers of vegetation type conversion in Southern California chaparral. *Ecosphere* **10**, e02796, doi:10.1002/ecs2.2796 (2019).

103 Lippitt C. L. *et al.* Influence of short-interval fire occurrence on post-fire recovery of fire-prone shrublands in California, USA. *Int. J. Wildland Fire* **22**, 184-193, doi:10.1071/WF10099 (2013).

104 Fusco, E. J. *et al.* Invasive grasses increase fire occurrence and frequency across US ecoregions, *Proc. Natl. Acad. Sci. U.S.A.* **116** (47), 23594-23599, doi:10.1073/pnas.1908253116 (2019).

105 Potts, J. B. & Stephens, S. L. Invasive and native plant responses to shrubland fuel reduction: comparing prescribed fire, mastication, and treatment season, *Biol. Conserv.* **142** (8), 1657-1664, doi: 10.1016/j.biocon.2009.03.001 (2009).

106 Shinneman, D. J. *et al.* The ecological uncertainty of wildfire fuel breaks: examples from the sagebrush steppe. *Front Ecol Environ* **17**(5): 279–288, doi:10.1002/fee.2045 (2019).

107 Burke, M. *et al.* Exposures and behavioral responses to wildfire smoke. *Nat. Hum. Behav.* **6**, 1351-1361, doi:10.1038/s41562-022-01396-6 (2022).

108 Miller, N. H., Molitor, D. & Zou, E. *The Nonlinear Effects of Air Pollution on Health: Evidence from Wildfire Smoke*. National Bureau of Economic Research Working Paper Series No. 32924, doi:10.3386/w32924 (2024).

109 Baggett, A. G. J. 3 San Joaquin Agric. L. Rev. *San Joaquin Agric. L. Rev.* **3**, 221-246 (1993).

110 Heard, S. & Franklin., B. *Building California's Forest Resilience Workforce: A Critical Gap In Increasing the Pace and Scale of Wildfire Prevention*. (The Nature Conservancy, 2023)

111 Wildfire safety: The California Wildfire Mitigation Strategic Planning Act., California Senate Bill 1014, (2024). https://legiscan.com/CA/text/SB1014/id/2915484/California-2023-SB1014-Introduced.html.

112 Clark, S.A. *et al*. Realignment of federal environmental policies to recognize fire's role. *fire ecol* **20**, 74, doi:10.1186/s42408-024-00301-y (2024).

113 Scott, Joe H. *et al.* Wildfire Risk to Communities: Spatial datasets of landscape-wide wildfire risk components for the United States. 2nd Edition. Fort Collins, CO: Forest Service Research Data Archive. doi:10.2737/RDS-2020-0016-2 (2024).

114 Li, F. *et al.* Historical (1700–2012) global multi-model estimates of the fire emissions from the Fire Modeling Intercomparison Project (FireMIP). *Atmos. Chem. Phys.* **19**, 12545-12567, doi:10.5194/acp-19-12545-2019 (2019).

115 Keller, C. A. *et al.* HEMCO v1.0: a versatile, ESMF-compliant component for calculating emissions in atmospheric models. *Geosci. Model Dev.* **7**, 1409-1417, doi:10.5194/gmd-7-1409-2014 (2014).

116 McDuffie, E. E. *et al.* A global anthropogenic emission inventory of atmospheric pollutants from sector- and fuel-specific sources (1970–2017): an application of the Community Emissions Data System (CEDS). *Earth Syst. Sci. Data* **12**, 3413-3442, doi:10.5194/essd-12-3413-2020 (2020).

117 Simone, N., Stettler, M., Eastham, S. & Barrett, S. *Aviation Emissions Inventory Code (AEIC) (2.0.0).* https://doi.org/10.5281/zenodo.6462261. 2012.

118 Guenther, A. B. *et al.* The Model of Emissions of Gases and Aerosols from Nature version 2.1 (MEGAN2.1): an extended and updated framework for modeling biogenic emissions. *Geosci. Model Dev.* **5**, 1471-1492, doi:10.5194/gmd-5-1471-2012 (2012).

119 Pai, S. J. *et al.* An evaluation of global organic aerosol schemes using airborne observations. *Atmos. Chem. Phys.* **20**, 2637-2665, doi:10.5194/acp-20-2637-2020 (2020).

120 Marrison, H., Penn, S. & Roman, H. *Review of Baseline Incidence Rate Estimates for Use in 2016 Socioeconomic Assessment*. (Industrial Economics, the South Coast Air Quality Management District, 2016).

121 Krewski, D. *et al. Extended Follow-Up and Spatial Analysis of the American Cancer Society Study Linking Particulate Air Pollution and Mortality*. (Health Effects Institute, Boston, Massachusetts, 2009).

122 Jerrett, M. *et al.* Spatial analysis of air pollution and mortality in California. *Am. J. Respir. Crit. Care Med.* **188**, 593-599, doi:10.1164/rccm.201303-0609OC (2013).

123 Economics, I. *Literature Review of Air Pollution-Related Health Endpoints and Concentration–Response Functions for Ozone, Nitrogen Dioxide, and Sulfur Dioxide: Results and Recommendations*. (Industrial Economics, Cambridge, MA 02140, 2016).

124 Economics, I. *Literature Review of Air Pollution-Related Health Endpoints and Concentration–Response Functions for Particulate Matter: Results and Recommendations*. (Industrial Economics, Cambridge, MA 02140, 2016).

125 Robinson, L. A. & Hammitt, J. K. Valuing Reductions in Fatal Illness Risks: Implications of Recent Research. *Health Econ.* **25**, 1039-1052, doi:10.1002/hec.3214 (2016).
126 Roman, H., Marrison, H. & Robinson, L. *A. Review of Morbidity Valuation Estimates for Use in 2016 Socioeconomic Assessment*. (Industrial Economics, 2016).
127 Roman, H. & Robinson, L. A. *Review of Mortality Risk Reduction Valuation Estimates for 2016 Socioeconomic Assessment*. (Industrial Economics, 2016).
128 Nandi, A. *et al.* Global and regional projections of the economic burden of Alzheimer's disease and related dementias from 2019 to 2050: A value of statistical life approach. *The Lancet* **51**, 101580, doi:10.1016/j.eclinm.2022.101580 (2022).
129 Lundberg, S. M. & Lee, S.-I. in *Proceedings of the 31st International Conference on Neural Information Processing Systems* 4768–4777 (Curran Associates Inc., Long Beach, California, USA, 2017).

Acknowledgments

We thank R. Bales for helpful discussions. **Funding:** J.C. and S.J.D. were supported by the ClimateWorks Foundation (grant 22-2100). A.P.W was supported by the Gordon and Betty Moore Foundation (grants 11974 and 13283). **Author contributions:** S.J.D. and M.G. conceived the study. J.C. and S.J.D. developed the methodological framework, with refinements by J.R. and A.P.W. J.C. conducted the simulations and analyses, utilizing input data partially provided by S.C. and Q.Z. J.C., S.J.D., and A.P.W. prepared the manuscript with contributions from all authors. S.J.D. directed the research. **Competing interests:** The authors declare that they have no known competing financial interests or personal relationships that could have appeared to influence the work reported in this paper.

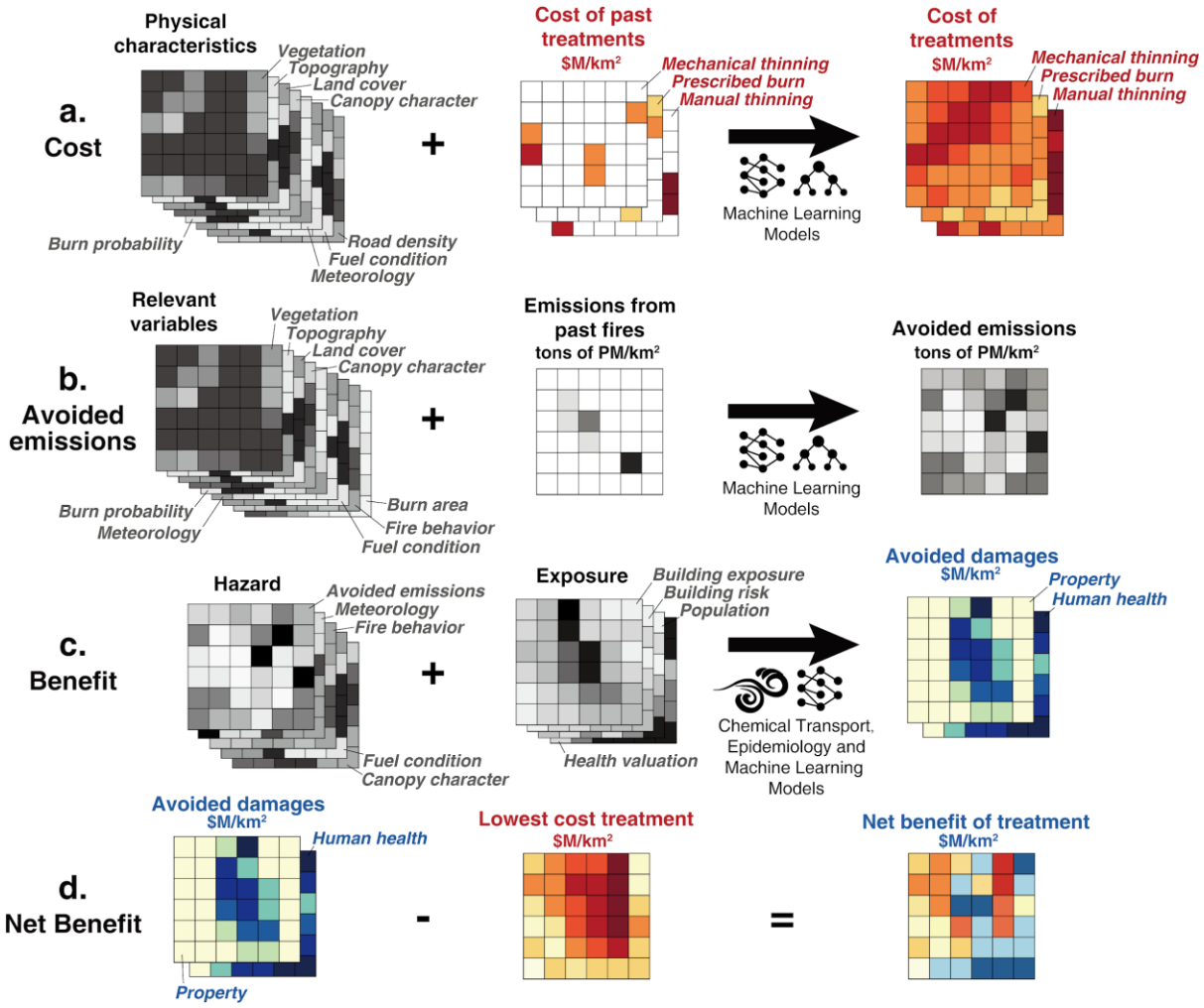

Fig. 1. Analytic approach. The net benefits of wildfire fuel treatments in California (**d**) were assessed by combining estimated treatment costs (**a**), projected fire emissions that might be avoided (**b**), estimated direct and indirect benefits of avoided damage to property and human health, respectively (**v**). In each case, analyses encompassed the entire state at a resolution of 0.01 degree (~1.11 km^2). Treatment costs and fire emissions were evaluated using machine learning methods and historical cost (USFS) and fire emissions (GFEDv4) datasets, along with datasets of vegetation, meteorology, topography, and historical fire characteristics. Indirect health benefits were evaluated using chemical transport (GEOS-Chem) and epidemiological (BenMAP-CE) models (see Methods and Table S2 for details).

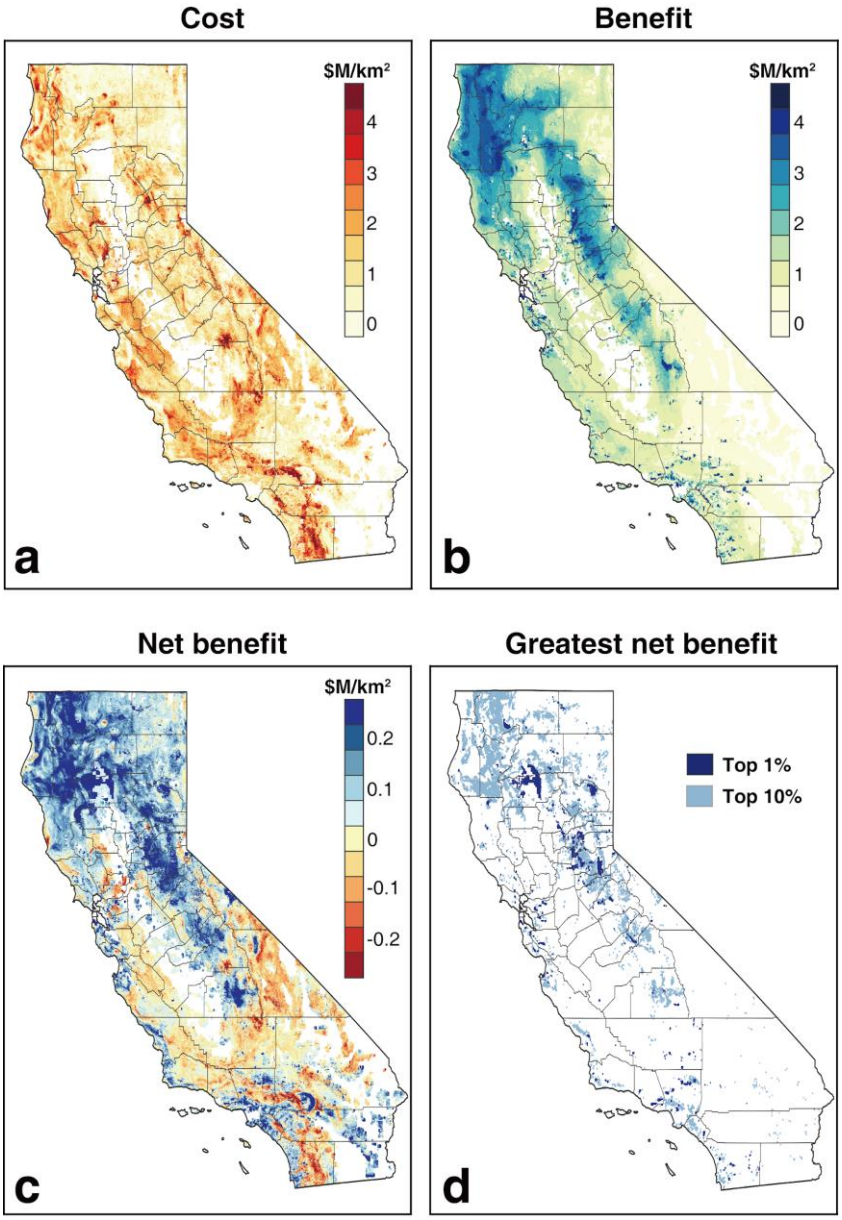

Fig. 2. Spatial distribution of treatment costs and benefits. Maps show the minimum cost of fuel treatments (**a**), combined benefits of avoided health damages and avoided property damage (**b**), net benefits (**b** minus **a**; **c**), and the areas with greatest 1% and 10% of net benefits (**d**).

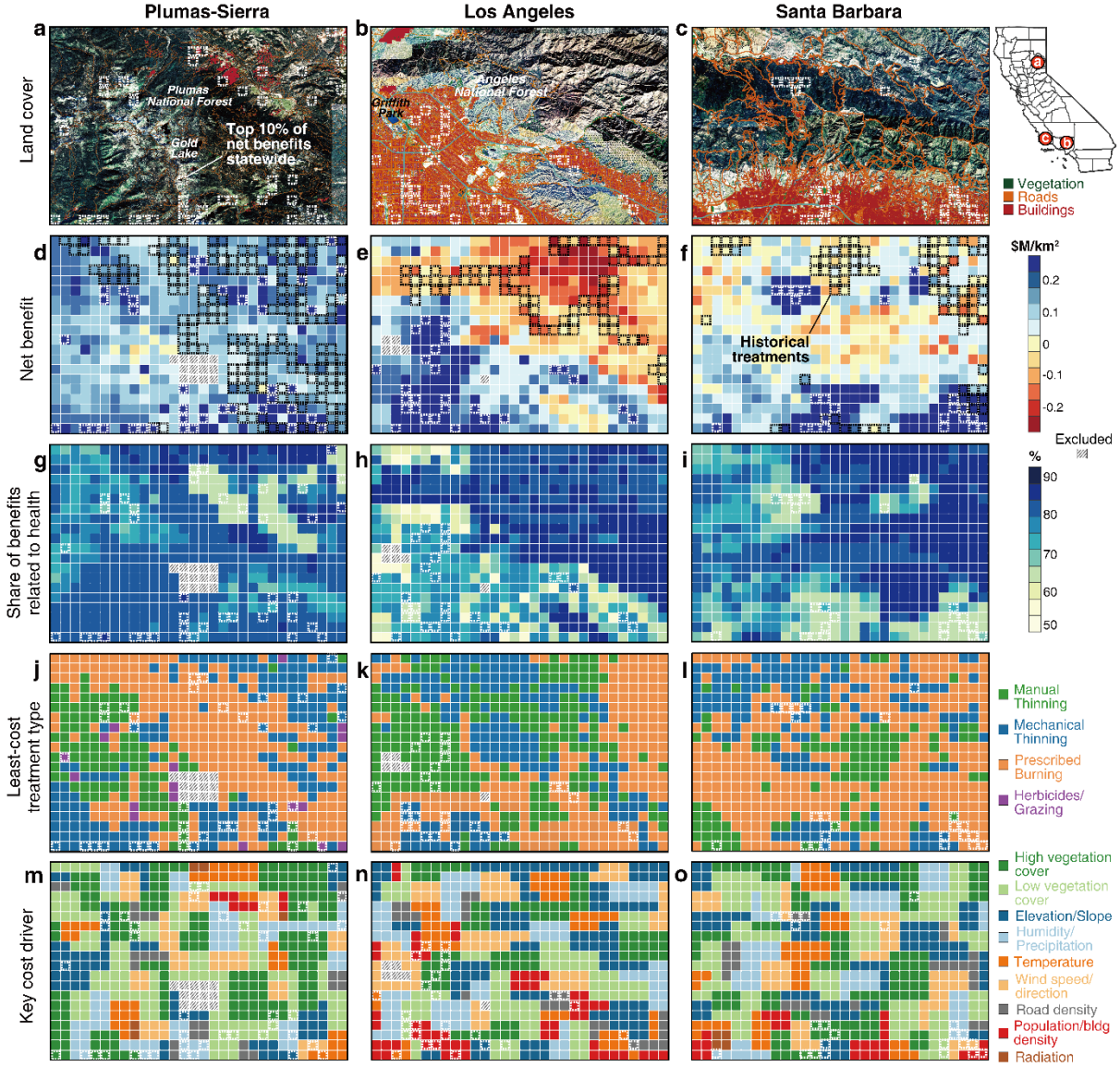

Fig. 3. Regional zoom-in view of treatment net benefits and dominant drivers across California. Remote sensing composite images illustrate land cover, terrain and urban structure in three representative regions with distinct ecological–urban contexts: forested (Plumas-Sierra; **a**), urbanized (Los Angeles; **b**), and mixed (Santa Barbara; **c**). Projected maps show: estimated net benefits of implementing fuel treatments, with black outlines indicating areas of historical treatment activity (**d-f**); the proportion of total benefits attributable to health-related smoke reduction (**g-i**); optimal treatment types selected to minimize treatment costs, including prescribed burn (PBurn), mechanical thinning (MechThin), manual thinning (ManThin), and other treatments (Other) (**j-l**); and the most influential predictive covariates driving treatment cost at each grid cell, derived from SHAP-based feature importance analysis (**m-o**).

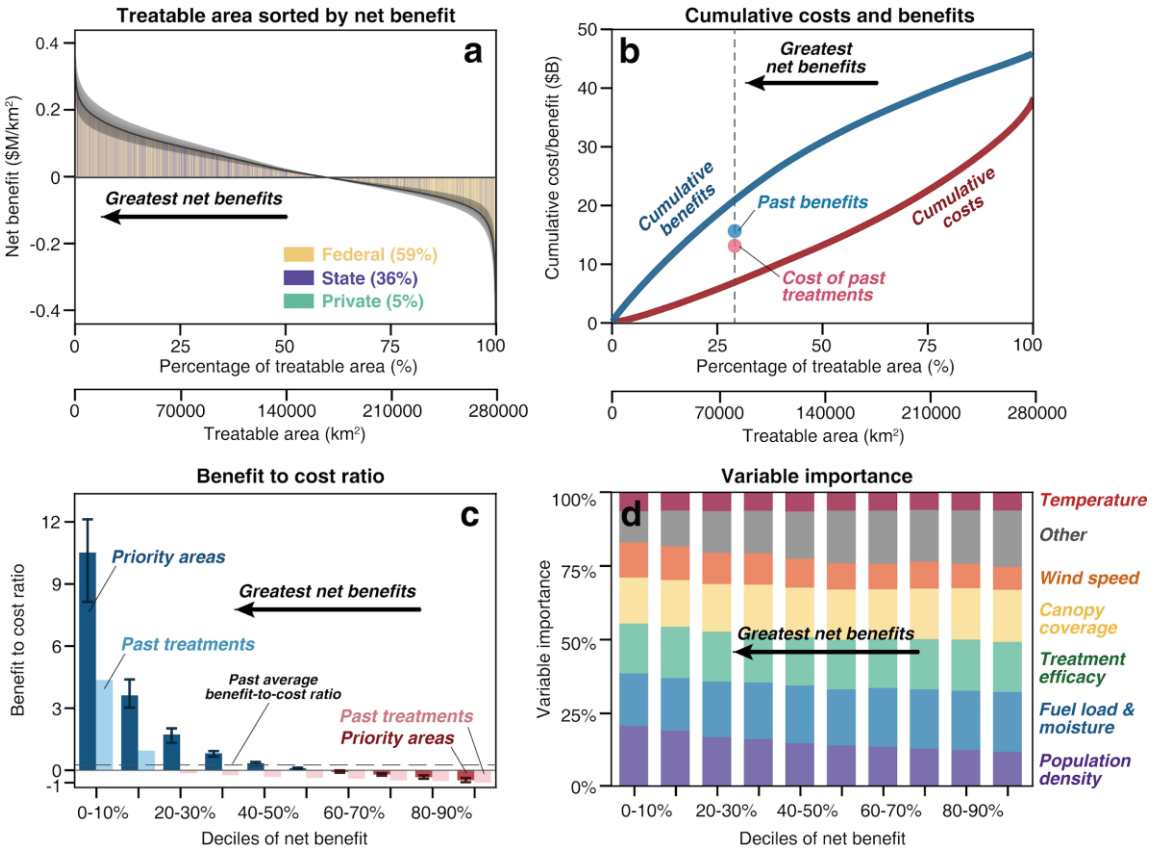

Fig. 4. Prioritizing fuel treatments. A majority (60%) of treatment areas have positive net benefits, exceeding $100k per km^2 in 30% the treatable areas (**a**). Past fuel treatments do not compare favorably in terms of the costs and benefits that are possible (**b** and **c**). Based on 5000 Monte Carlo simulations, areas with the greatest estimated net benefits are most sensitive to population density, fuel load, treatment efficacy and canopy coverage, (**d**).

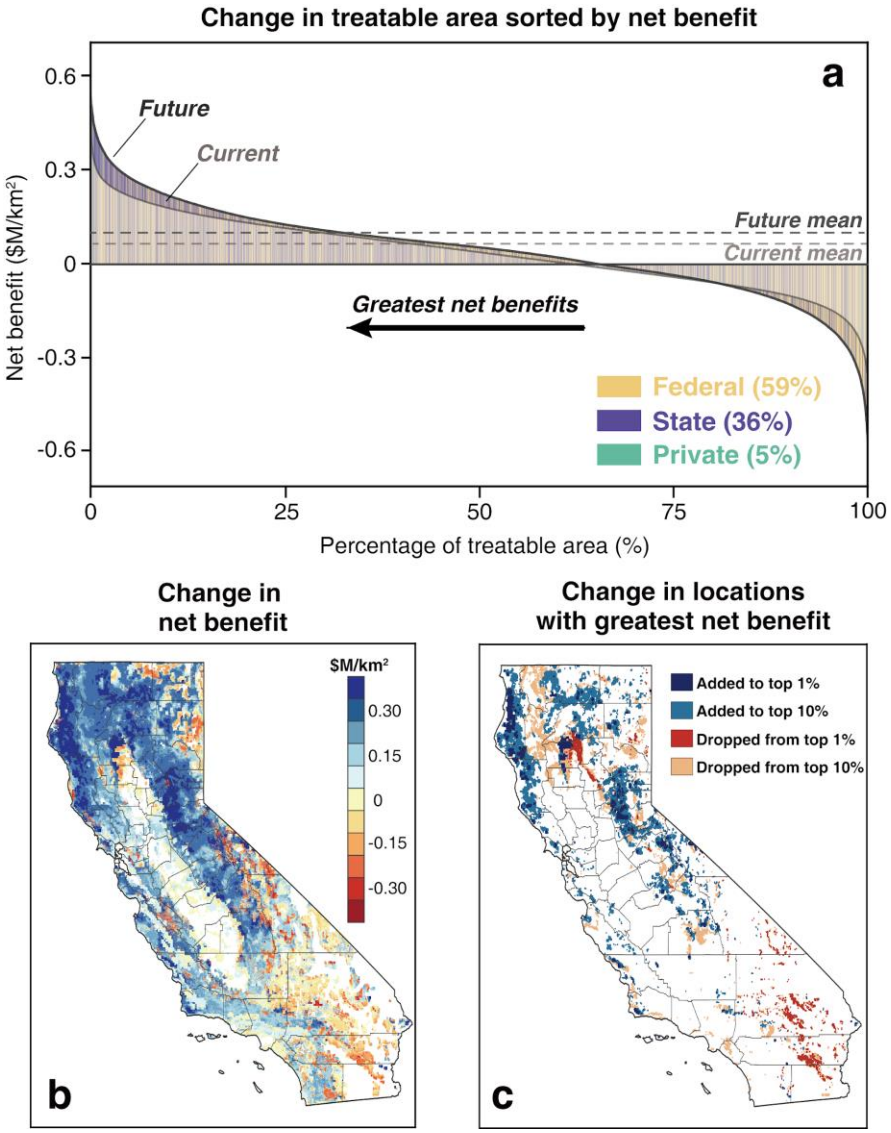

Fig. 5. Changes in net benefits of fuel treatments under climate change. The share of treatable areas with positive net benefits increases modestly by 2050 under the SSP245 scenario of climate change (**a**), and these changes are geographically heterogenous (**b** and **c**). These changes do not include projected changes in population or building density, only fire risk, emissions, and treatment costs.